Appl. Phys. 9, 179–204 (1976)

Applied Physics

Superconductivity

A Probe of the Magnetic State of Local Moments in Metals*

*M. Brian Maple***
Institute for Pure and Applied Physical Sciences
University of California, San Diego, La Jolla, CA 92093, USA

Received 29 August 1975/Accepted 18 November 1975

Abstract. The superconducting and normal state properties are reviewed for exemplary matrix-impurity systems in the three distinct regimes of magnetic character of the impurity which have been identified. It is shown that these three regimes can be distinguished by the *detailed* behavior of the depressions of 1) the superconducting transition temperature T_c as a function of impurity concentration n and 2) the specific heat jump ΔC at T_c as a function of T_c. These systematics of superconductivity in the presence of local moments appear to be sufficiently well established that it is possible to 1) ascertain whether the solute spin is long-lived (magnetic) or short-lived (nonmagnetic) compared to thermal fluctuation lifetimes at superconducting temperatures, 2) determine the sign and magnitude of the conduction electron-impurity spin exchange interaction parameter $\mathcal{J}$ and the temperature dependence of the exchange scattering of conduction electrons by *long-lived* solute spins, 3) derive, in favorable cases, information pertaining to the energy level structure of rare earth ions in the crystalline electric field of their superconducting metallic host, and 4) observe magnetic-nonmagnetic transitions of an impurity induced by the application of an external pressure or variation of the composition of a binary alloy matrix.

Traditionally, efforts to delineate the magnetic state of an impurity in a metallic host have relied upon the comparison of measurements of various normal state physical properties as a function of temperature and magnetic field with predictions based on available theoretical models. However, this approach suffers from two drawbacks. First, a meaningful comparison between experiment and theory requires that the temperature and field dependence of the impurity contribution to the physical properties of the matrix-impurity system be determined in the single impurity limit. In order to realize this limit where the impurity contribution depends linearly on impurity concentration, it is necessary to reduce the impurity concentration to a level that is sufficiently low so as to avoid inter-impurity interaction effects, but concomitantly, achieve adequate sensitivity to allow the sought after variation of the normal state physical properties with temperature and field to be accurately deduced after the large background of the matrix has been subtracted from the alloy. Often, it is also necessary to account for modifications of the host properties which accompany the introduction of impurities that arise from scattering processes other than those of magnetic origin (e.g., the breakdown of Matthiesen's rule for the electrical resistivity is a case in point). Second, theories based on competing mechanisms sometimes simply yield the same theoretical predictions for the temperature and field dependence of the normal state physical properties, so that it is not possible to distinguish which is appropriate for the situation

* This article is based upon an invited presentation at the 1973 Summer meeting of the American Physical Society in East Lansing, Michigan, 18–20 June 1973 [Bull. Amer. Phys. Soc. 18, 779 (1973)].

** Supported by the U.S. Energy Research and Development Administration under Contract No. ERDA E(04-3)-34 PA 227.

under consideration. Fortunately, these difficulties can be obviated to a large extent by measuring the superconducting properties of the matrix-impurity system when the matrix is a superconductor.

The advantage which superconducting studies offer in determining the magnetic state of impurities when the metallic matrices into which they have been introduced are superconducting derives from the extreme sensitivity of the superconducting electron gas to the presence of localized impurity states. The resulting modifications of the superconducting order parameter and energy gap are reflected in the superconducting properties, often in dramatic ways. In particular, striking nonlinear variations are observed in the depressions of 1) the superconducting transition temperature T_c as a function of solute concentration n and 2) the specific heat jump ΔC at T_c as a function of T_c. Both are replete with information, not contained in the normal state properties, pertaining to the mechanisms through which the superconducting electron pairs interact with the solute moments, and in turn, the magnetic state of the solutes. Moreover, these measurements can be performed with relative ease without the necessity of making large background corrections for the host, and in many cases, the effects are so pronounced that inter-impurity interactions can even be neglected if they are not too strong. The main disadvantage associated with the application of this "superconducting spectroscopy" in determining the magnetic state of impurities in metallic matrices is, of course, the requirement that the matrix be a superconductor.

In this article we wish to show that impurity ions with partially-filled d or f shells affect the superconductivity of the metallic matrix into which they have been dissolved in a distinct manner which correlates with their own magnetic state. Two distinguishing features to be observed in the superconductivity of a matrix-impurity system which we emphasize are the *detailed* behaviors of the curves of T_c/T_{c_0} vs n and $\Delta C/\Delta C_0$ vs T_c/T_{c_0} (T_{c_0} and ΔC_0 refer to the matrix). By reviewing the superconducting and normal state properties of exemplary systems which have been extensively studied in various regimes of solute magnetic character, we show that the systematics of superconductivity in the presence of local moments appear to be sufficiently well established to permit the magnetic state of a solute in a superconducting metal to be determined from superconducting properties alone. Specifically, we demonstrate that it is possible to 1) ascertain whether the solute spin is long-lived (magnetic) or short-lived (nonmagnetic) compared to thermal fluctuation lifetimes at superconducting temperatures, 2) determine the sign and magnitude of the conduction electron-impurity spin exchange interaction parameter $\mathcal{J}$ and the temperature dependence of the exchange scattering of conduction electrons by *long-lived* solute spins, 3) derive, in favorable cases, information pertaining to the energy level structure of rare earth (RE) ions in the crystalline electric field of their superconducting metallic host, and 4) observe magnetic-nonmagnetic transitions of an impurity induced by the application of an external pressure or variation of the composition of a binary alloy matrix.

It should be pointed out that our review of the superconducting and normal state properties of the exemplary matrix-impurity systems considered is not meant to be comprehensive; other reviews have recently appeared [1–5], and our main purpose is to stress the applicability of superconductivity to probe the magnetic state of local moments in metals. The breakdown of the article is as follows: In Section 1, we present our classification of local moments in metals and discuss the systematics of superconductivity in the presence of local moments. Section 2 is devoted to magnetic-nonmagnetic transitions of impurities in superconductors; while Section 3 considers superconductors containing rare earth impurities with crystal-field split energy levels. The article is concluded in Section 4.

1. The Systematics of Superconductivity in the Presence of Local Moments

In this section, we review the superconducting properties of matrix-impurity systems in the three *distinct* categories which have been identified, each of which corresponds to a different regime of solute magnetic character. Before presenting these systematics of superconductivity in the presence of local moments, however, it is first necessary to introduce the scheme which we employ to classify local moments in a metal with respect to their magnetic character.

1.1. Classification of Local Moments in Superconductors

In the traditional view, the formation of local moments in metals is intimately connected with the extent to which the conduction electron wave functions hybridize with the localized d or f impurity wave

functions. As a result of this admixture of itinerant and local electrons, the lifetime τ of an electron in the localized state is finite (rather than infinite as it would be for an unhybridized local d or f state). The lifetime τ is given by

$$\tau^{-1} = \pi\hbar^{-1}\langle V_{kl}^2\rangle N(E_F), \tag{1}$$

where V_{kl} is the itinerant-local electron admixture matrix element and $N(E_F)$ is the density of states at the Fermi level for the matrix. A finite lifetime τ in turn implies a broadening of the localized impurity state in energy by an amount of the order of $\hbar/\tau$. According to the Friedel-Anderson model [6, 7], the local density of states $N_l(E_F)$ at the Fermi level associated with the broadened localized state which each solute ion contributes has a Lorentzian form

$$N_l(E_F) = \frac{1}{\pi}\frac{\Delta}{E_l^2+\Delta^2} \tag{2}$$

(without spin and orbital degeneracy),

where E_l is the energy separating the centroid of the resonant impurity state and the Fermi level E_F and Δ is the Hartree-Fock half-width of the resonant impurity state. In this view, whether or not a solute forms a local moment is determined by a competition between Δ and the intra-atomic Coulomb repulsion U which splits spin-up and spin-down states in the Friedel-Anderson model. This is illustrated by the Hartree-Fock condition for spin degeneracy (no magnetic moment) which is given by

$$N_l(E_F)U \leqq 1. \tag{3}$$

When the centroid of the resonant impurity state is located at the Fermi level ($E_l = 0$), this criterion reduces to the more familiar relation

$$U/\pi\Delta \leqq 1. \tag{4}$$

Thus, according to the Friedel-Anderson model, a solute in a matrix-impurity system is more likely to carry a local moment the larger the value of U and the smaller the value of Δ. Since Δ is proportional to $\langle V_{kl}^2\rangle$, it is apparent that the amount of itinerant-local electron mixing is an important determinant in the formation of solute local moments in a metallic environment.

Actually, the abrupt transition from magnetism to nonmagnetism at $U/\pi\Delta = 1$ predicted by the Friedel-Anderson model does not occur in the dilute impurity limit. Instead, the magnetic-nonmagnetic transition seems to be a smooth function of $U/\pi\Delta$ (or other related factors—see Section 2), and a great deal of effort has been expended in attempting to develop a theoretical description of the transition [8, 9]. One approach (and by no means the only one) is based on the concept of a localized spin fluctuation lifetime τ_{sf} which is a smooth function of $U/\pi\Delta$. The long-lived local moment (magnetic) limit corresponds to $U/\pi\Delta \gg 1$ and the short-lived local moment (nonmagnetic) limit corresponds to $U/\pi\Delta \ll 1$ where τ_{sf} is expected to be of the order of the lifetime τ of an electron in the localized state. Again, the amount of itinerant-local electron mixing is an important factor in determining the lifetime of the solute local moment and, in turn, the solute's magnetic character.

Although a detailed discussion is beyond the scope of this article, we feel obliged to remark at this point that the "valence fluctuation" model [10–12] which incorporates the concept of temporal fluctuations of a partially filled localized electron shell between two integrally occupied states provides a natural explanation of the local moment fluctuations considered here. This model has recently been invoked to explain the nonmagnetic behavior and non-integral valence of certain RE ions in metallic environments [11, 12]. Indeed, the nonmagnetic nature of Ce impurities in Th, which was first discovered through measurements in the superconducting state [13, 14] (an example of the utility of superconductivity as a probe of the magnetic state of an impurity in a metal), correlates with a nonintegral occupation (0.75 electrons) of the Ce $4f$ shell.

Our classification of local moments in metals is based on the notion that the solute spins fluctuate with a finite frequency τ_{sf}^{-1} and that the lifetime τ_{sf} is inversely related to the extent to which the localized impurity states hybridize with the conduction electron states of the matrix. In this view, a solute is magnetic in the limit where τ_{sf} is large compared to thermal fluctuation lifetimes $\tau_{th} \sim \hbar/k_B T$ in the temperature range of interest (i.e., $\tau_{sf} \gg \tau_{th}$) and nonmagnetic in the opposite limit (i.e., $\tau_{sf} \ll \tau_{th}$). Two of the three distinct categories of solute magnetic character for superconducting matrix-impurity systems correspond to the magnetic limit where the solute spins are long-lived compared to thermal fluctuation lifetimes at superconducting temperatures ($\tau_{sf} \gg \hbar/k_B T_{c_0}$ or $T_0 \ll T_{c_0}$), while the third distinct category corresponds to a nonmagnetic limit where the solute spins are short-lived compared to thermal fluctuation lifetimes at superconducting temperatures ($\tau_{sf} \ll \hbar/k_B T_{c_0}$ or $T_0 \gg T_{c_0}$). Here, we have introduced the localized spin

fluctuation temperature T_0 which is defined as $T_0 \equiv \hbar/k_B\tau_{sf}$. In the long-lived magnetic limit, the solute spins apparently interact with the conduction electrons via the conduction electron-impurity spin exchange interaction Hamiltonian

$$\mathscr{H} = -2\vartheta S \cdot s, \tag{5}$$

where ϑ is the parameter which characterizes the strength and sign of the interaction, S is the solute spin, and s is the conduction electron spin density at the impurity site. The first two categories are distinguished by the sign of ϑ, which is positive for weak itinerant-local electron mixing, and negative for moderate itinerant-local electron mixing. In the short-lived nonmagnetic limit, where there is strong itinerant-local electron mixing, the exchange interaction is apparently left inoperative by the rapid fluctuations of the solute moments. These three distinct categories are discussed in the following where the systematics of superconductivity in the presence of local moments are presented.

1.2. Long-Lived Local Moments in Superconductors ($T_0 \ll T_{c_0}$)

1.2.1. Weak Itinerant-Local Electron Mixing ($\vartheta > 0$)

When the admixture of conduction electron and localized impurity states is weak, the lifetime of an electron in the localized impurity state remains, for all practical purposes, infinite. The electronic structure of the local shell then retains its highly correlated atomic identity and the resultant magnetic moment, dictated by Hund's rules, interacts with the conduction electrons via the conduction electron-impurity spin exchange Hamiltonian. This case is especially appropriate for RE ions whose $4f$ shells have radii which are only about one-tenth of a typical interatomic crystal spacing, although some notable exceptions (in particular, Ce) will be considered in ensuing sections. In this weak itinerant-local electron mixing limit, the Heisenberg contribution ϑ_0 to the exchange interaction parameter ϑ dominates so that ϑ is given by

$$\vartheta \sim \vartheta_0 = -\int \phi_{4f}^*(r_2)\psi_k^*(r_1)\frac{e^2}{r_{12}}\phi_{4f}(r_1)\psi_k(r_2)d^3r_1 d^3r_2, \tag{6}$$

where ψ_k is the conduction electron wave function, and ϕ_{4f} is the localized $4f$ electron wave function. This Heisenberg contribution to ϑ is always positive (ferromagnetic coupling). We remark that for RE impurities, the appropriate exchange Hamiltonian is

$$\mathscr{H}_{\text{int}} = -2\vartheta(g_J - 1)J \cdot s \tag{7}$$

which is obtained by replacing S in (5) by its projection onto the total angular momentum vector $J = L + S$ of the Hund's rule ground state (i.e., $S \rightarrow [\langle S \cdot J\rangle / J(J+1)]J = (g_J - 1)J$ where g_J is the Lande g-factor for the appropriate Hund's rule ground state) [15, 16].

In this section we will further restrict our attention to the S-state RE ion Gd since there is no appreciable splitting of the Gd^{3+} $J = 7/2$ multiplet in the cubic crystal field of the superconducting matrices which we consider. The interesting and varied effects on superconductivity which arise when RE impurities with crystal-field split energy levels are dissolved in a superconducting matrix will be considered in Section 3. As an exemplary matrix-impurity system, we consider the system (LaGd)Al_2.

Exemplary System—(LaGd)Al_2. The normal state properties of the (LaGd)Al_2 system reveal that the Gd moment is long-lived and that the conduction electron-impurity spin exchange parameter ϑ is positive. For example, magnetic studies [17, 18] show that the magnetic susceptibility χ of (LaGd)Al_2 follows a Curie-Weiss law

$$\chi = N\mu_{\text{eff}}^2/3k_B(T - \theta) \tag{8}$$

at low temperatures. The Curie-Weiss temperatures θ are close to the Curie temperatures θ_f of those samples which order ferromagnetically above a critical concentration which is somewhat above the critical concentration for the complete suppression of superconductivity. The conformation of the susceptibility to a Curie-Weiss law indicates that the moment is long-lived, while the enhanced value of μ_{eff} ($\sim 9\mu_B$ compared to the free ion value of $7.94\,\mu_B$) suggests a positive conduction electron polarization and, in turn, a positive sign for ϑ. The absence of a minimum in the low temperature electrical resistivity of (LaGd)Al_2 alloys also suggests that ϑ is positive. Direct evidence that ϑ is positive has recently emerged from an electron paramagnetic resonance study of the (LaGd)Al_2 system [19]. In this study it was found that (LaGd)Al_2 is a "bottlenecked" system. When the "bottleneck" is broken by reducing the Gd concentration or by adding chemical impurities, there is a positive g-shift of 0.1 which corresponds to a value for ϑ of ~ 0.1 eV.

Experimentally, it has been found that when interactions between Gd impurities are sufficiently weak

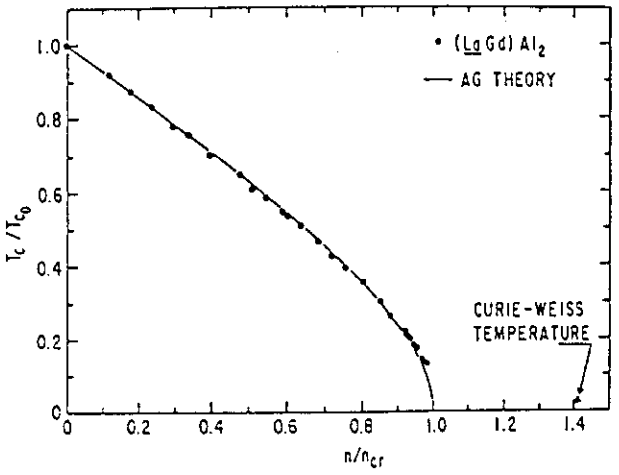

Fig. 1. Reduced transition temperature T_c/T_{c_0} vs reduced concentration n/n_{cr} for (LaGd)Al_2 compared to the AG theory (solid curve). $T_{c_0} = 3.24$ K and $n_{cr} = 0.590$ at.-% Gd substitution in La. The reduced Curie-Weiss temperature θ/T_{c_0} measured at $n/n_{cr} = 1.41$ is denoted by the solid triangle (after Maple [20])

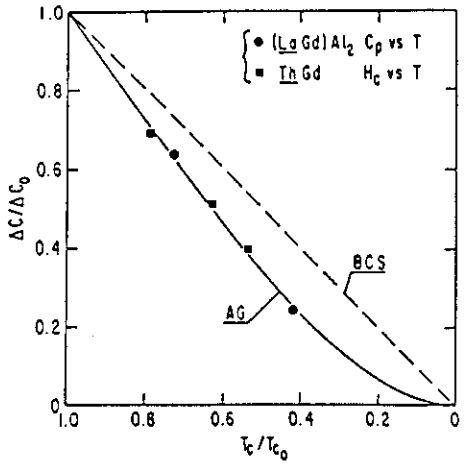

Fig. 2. Reduced specific heat jump $\Delta C/\Delta C_0$ vs reduced transition temperature T_c/T_{c_0} for the matrix-impurity systems (LaGd)Al_2 and ThGd. The (LaGd)Al_2 data were derived from measurements of C_p vs T by Luengo and Maple [21] and the ThGd data were derived from measurements of H_c vs T by Decker and Finnemore [23]. The dashed line represents the BCS law of corresponding states, whereas the solid line is the result of the AG theory as calculated by Skalski *et al.* [24]

that they may be neglected over an appreciable temperature range below T_{c_0}, the transition temperature of the superconducting matrix into which they have been dissolved, then the curves of T_c/T_{c_0} vs n/n_{cr} (n_{cr} is the critical concentration above which superconductivity does not occur at any temperature [17, 20]) and $\Delta C/\Delta C_0$ vs T_c/T_{c_0} [21] behave in characteristic manners, both of which can be well-represented by universal functions which have been calculated on the basis of the theory of Abrikosov and Gor'kov [22] (hereafter AG) as discussed below. This is illustrated in Figs. 1 and 2. In Fig. 1, the behavior of T_c/T_{c_0} vs n/n_{cr} [17, 20] is displayed for the exemplary system (LaGd)Al_2 and compared to the theoretical AG curve (solid line in the figure). The solid triangle in Fig. 1 represents the Curie-Weiss temperature θ measured for a sample with a Gd concentration well above the critical concentration n_{cr} which indicates that interaction effects are indeed weak in the temperature range (or impurity concentration range) over which experiment has been compared with theory. In Fig. 2, the behavior of $\Delta C/\Delta C_0$ vs T_c/T_{c_0} [21] is shown for the (LaGd)Al_2 system and another system, ThGd [23], and compared to calculations by Skalski *et al.* [24] which are based on the AG theory. For the ThGd system, the specific heat jumps have been derived from critical field measurements by means of Rutger's relation

$$\Delta C = C_s - C_n = (vT/4\pi)\,(dH_c/dT)^2_{T=T_c}\,, \tag{9}$$

where v represents the volume of the superconducting specimen.

Temperature Independent Pair Breaking. As can be seen in Figs. 1 and 2, the experimental T_c/T_{c_0} vs n/n_{cr} and $\Delta C/\Delta C_0$ vs T_c/T_{c_0} curves are well represented by the AG theory. The basic assumptions embodied in the AG theory are that 1) the superconducting order parameter does not vary with position, 2) the spins of the impurities are fixed and randomly oriented in space, and 3) the scattering of conduction electrons by magnetic impurity spins can be calculated within the first Born approximation. The first assumption requires that the impurities be randomly distributed throughout the superconducting matrix, while the second precludes any correlations between the spins of the impurities such as those which would arise from magnetic order.

In the AG theory, the superconducting properties in the presence of solute spins are characterized by a pair breaking parameter $\alpha = \tau_s^{-1}$ where τ_s is the lifetime of the single particle paired states of which the superconducting wave function is comprised. The theory predicts a second order transition to the superconducting state and a rapid decrease of the transition temperature with α given by the universal relation

$$\ln(T_c/T_{c_0}) = \psi(1/2) - \psi(1/2 + 0.14\alpha T_{c_0}/\alpha_{cr} T_c)\,, \tag{10}$$

where T_{c_0} corresponds to $\alpha=0$, $\alpha_{cr}=k_B T_{c_0}/4\hbar\gamma$ ($\ln\gamma$ is Euler's constant) corresponds to $T_c=0$ (complete destruction of superconductivity), and ψ is the digamma function. It is apparently sufficient to calculate the pair breaking parameter α within the first Born approximation (to second order in ϑ) which gives the result

$$\alpha=\hbar^{-1}nN(E_F)\vartheta^2 S(S+1)\,, \tag{11}$$

where n is the paramagnetic impurity concentration and $N(E_F)$ is the density of states at the Fermi level for the matrix. It is important to note that α is *proportional to* n and *independent of temperature*. Hence α/α_{cr} can be replaced by n/n_{cr} in (10) where n_{cr} is the critical concentration for the complete suppression of superconductivity. Thus the theory predicts that the reduced transition temperature T_c/T_{c_0} will be a universal function of reduced concentration n/n_{cr}:

$$\ln(T_c/T_{c_0})=\psi(1/2)-\psi(1/2+0.14nT_{c_0}/n_{cr}T_c) \tag{12}$$

or

$$T_c/T_{c_0}=\mathcal{U}(n/n_{cr})\,. \tag{13}$$

The specific heat jump ΔC at T_c as a function of T_c has also been calculated on the basis of the AG theory by Skalski *et al.* [24]. They find that the reduced specific heat jump $\Delta C/\Delta C_0$ as a function of T_c/T_{c_0} follows another universal function

$$\Delta C/\Delta C_0=\mathcal{V}(T_c/T_{c_0}) \tag{14}$$

which deviates markedly from the linear BCS law of corresponding states [25] as expressed by

$$\Delta C/\Delta C_0=T_c/T_{c_0}\,. \tag{15}$$

Other predictions of the AG theory have been verified experimentally as outlined in a recent review [2].

1.2.2. Moderate Itinerant-Local Electron Mixing ($\vartheta<0$ and $T_K\ll T_{c_0}$)

When the admixture of conduction electron and localized impurity states is moderately strong (but not too strong), an electron in the local state still remains long-lived compared to thermal fluctuation lifetimes at superconducting temperatures. Again, the electronic structure of the local shell retains, to a high degree of approximation, its highly correlated atomic identity and the resultant magnetic moment, given by Hund's rules, interacts with conduction electrons via the conduction electron-impurity spin exchange Hamiltonian. In this case, however, the exchange interaction parameter ϑ is dominated by an anti-ferromagnetic contribution ϑ_1 which arises from covalent mixing so that ϑ is negative [26]. According to Schrieffer and Wolf [27], this contribution can be expressed in terms of the parameters of the Friedel-Anderson model as

$$\vartheta\sim\vartheta_1=\frac{\langle V_{kl}^2\rangle U}{E_l(E_l+U)}\,;\quad |E_l|\ll\Delta\,. \tag{16}$$

Matrix-impurity systems which fall into this category exhibit the Kondo effect [28] which is associated with a temperature dependent exchange scattering of conduction electrons by the long-lived solute spins. Calculated terms of the scattering cross-section of higher order than ϑ^2 become important when ϑ is negative, giving rise to various anomalies in the normal state. For example, there is an impurity contribution to the electrical resistivity which varies as $(-\ln T)$ for $T\gg T_K$ and saturates to a constant value (the so-called unitarity limit) for $T\ll T_K$ and produces the resistivity minimum phenomenon which was first explained by Kondo [29]. In addition, there are heat capacity and thermoelectric power anomalies which exhibit peaks near T_K. Here, T_K is the Kondo temperature which is given by

$$T_K\sim T_F\exp(-1/N(E_F)|\vartheta|)\,, \tag{17}$$

where T_F is the Fermi temperature. Much theoretical effort has been expended in attempting to calculate the various normal state properties of Kondo systems for all temperatures $T\gtrless T_K$. One physical interpretation which has emerged from these theories is that T_K is a characteristic temperature below which the impurity spins tend to be compensated by the conduction electron spins—the degree of compensation increasing smoothly with decreasing temperature. The binding energy of this so-called "quasi-bound state" is of the order of $k_B T_K$. The impurities which fall into this category include the $3d$ (Fe group) transition metals and certain rare earths, like Ce and Yb, depending, of course, on the electronic structure of the metallic host into which they have been introduced. As an exemplary system, we consider the matrix-impurity system (LaCe)Al_2.

Exemplary System—(LaCe)Al_2. The first matrix-impurity system in which a Kondo effect was observed where the metallic matrix was a compound rather than an element was (LaCe)Al_2 [17, 30]. The temperature dependent anomalies in the normal state physical properties of this system reveal that the Kondo temperature $T_K\sim 0.1$ K is much smaller than

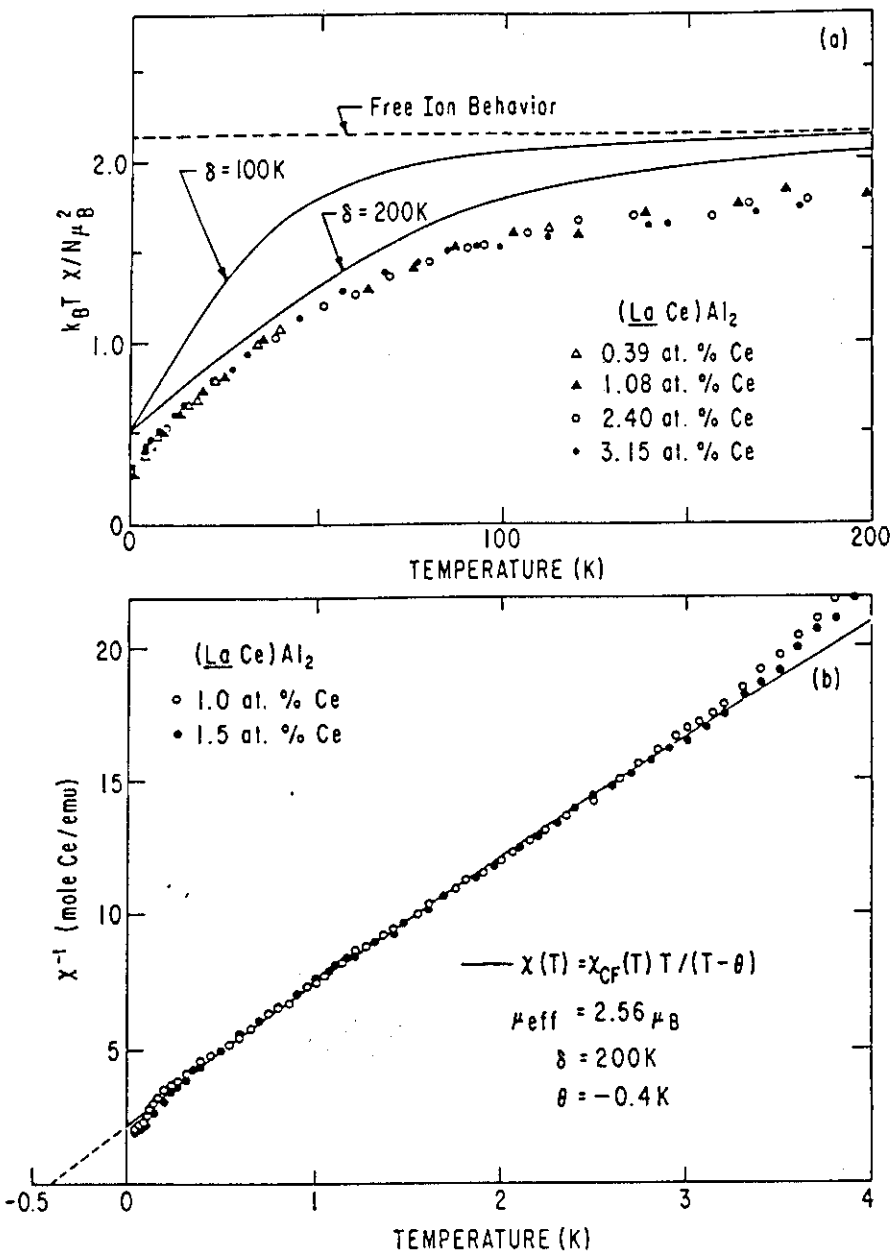

Fig. 3. (a) χT vs T plot of the magnetic susceptibility (corrected for the susceptibility of $LaAl_2$) of (LaCe)Al_2 alloys. The dashed line gives the value for free Ce^{3+} ions for which $k_B T\chi/N\mu_B^2 = g^2 J(J+1)/3 = 2.14$. The solid curves represent the susceptibility appropriate to a cubic crystal field which splits the Ce^{3+} $J = 5/2$ multiplet into a Γ_8 quartet and a ground state Γ_7 doublet (after Maple [17, 30]). (b) Inverse magnetic susceptibility (corrected for the susceptibility of $LaAl_2$) vs temperature for two (LaCe)Al_2 alloys below 4 K. The solid line represents a modified Curie-Weiss law with a temperature dependent Curie constant $C(T) = \chi_{CF}(T)T$ where $\chi_{CF}(T)$ is the susceptibility for a Γ_7–Γ_8 splitting δ of 200 K in the cubic crystal field (after Felsch *et al.* [33])

the critical temperature of the $LaAl_2$ host ($T_{c_0} = 3.3$ K). High temperature (1 K $< T <$ 200 K) magnetic susceptibility measurements on the (LaCe)Al_2 system suggest that the Ce^{3+} $J = 5/2$ Hund's rule multiplet is split by the cubic crystal field ($LaAl_2$ has the fcc C 15 crystal structure) into a Γ_8 quartet and a ground state Γ_7 doublet with a splitting $\delta \sim 10^2$ K [17, 30, 31]. This is illustrated in Fig. 3a where magnetic susceptibility data [17, 30] in the form of χT vs T plots for several (LaCe)Al_2 alloys are compared with theoretical curves for δ values of 0 (Curie law), 100 and 200 K. A more satisfactory description of the data presented in Fig. 3a has recently been obtained by Harris and Zuckermann [32] who have taken both crystal field and Kondo effects into consideration in their calculation of the magnetic susceptibility as a function of temperature. The best fit of their theory to the data corresponds to the reasonable values for $|\vartheta|$ and δ of 0.15 eV and 180 K, respectively. Low temperature (0.04 K $< T <$ 4 K) magnetic susceptibility measure-

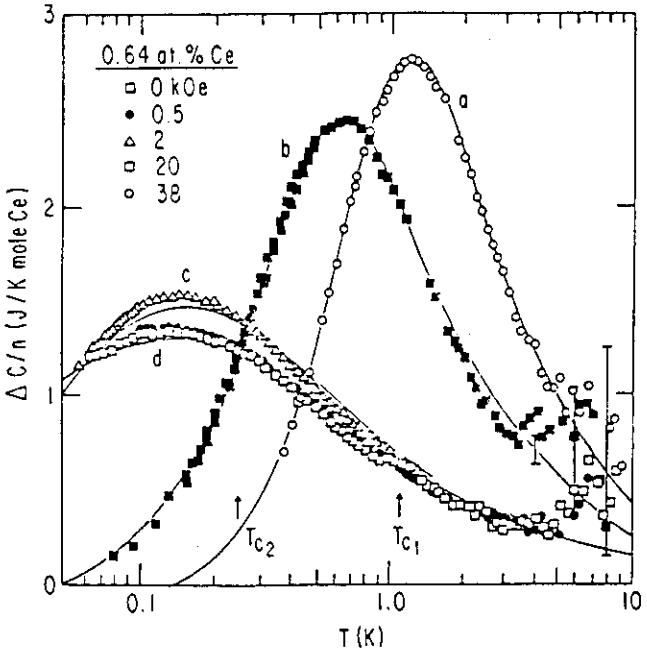

Fig. 4. Heat capacity of a (LaCe)Al_2 alloy (0.64 at.-% Ce) vs temperature in various magnetic fields up to 38 kOe. Curves *a*–*c*, which have been drawn to fit more accurate data for a (LaCe)Al_2 alloy with 0.906 at.-% Ce, correspond to an entropy of $R \ln 2$ per mole Ce, showing that the Ce^{3+} ground state is a doublet. Curve *d* is consistent with calculations of Bloomfield and Hamann [36] for $S = 1/2$ and $T_K = 0.42$ K. The two zero field superconducting transition temperatures are indicated (after Bader *et al.* [34])

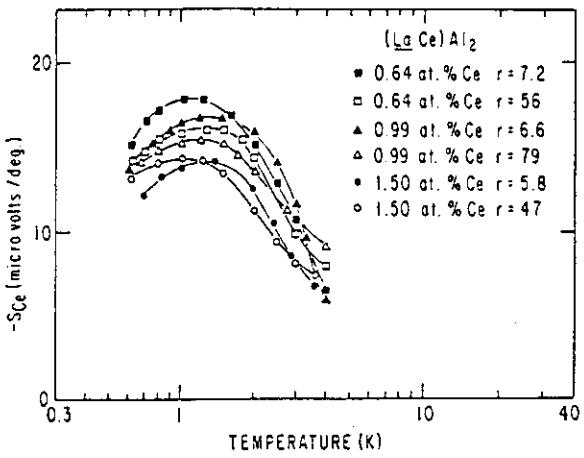

Fig. 5. Negative thermoelectric power contributed by Ce impurities in various (LaCe)Al_2 alloys as determined from the Gorter-Nordheim relation. The symbol *r* denotes the resistance ratio $R(300\,K)/R(12\,K)$ of each specimen (after Moeser *et al.* [38])

ments on the (LaCe)Al_2 system suggest that T_K is of the order of 0.1 K [33]. This is shown in Fig. 3b where inverse magnetic susceptibility vs temperature data for two (LaCe)Al_2 alloys have been fitted by a modified Curie-Weiss law with a temperature dependent Curie constant $C(T) = \chi_{CF}(T)T$ where $\chi_{CF}(T)$ is the susceptibility for a $\Gamma_7 - \Gamma_8$ splitting δ of 200 K [33]. Here, the 0.4 K Curie-Weiss temperature θ is taken to be a measure of T_K (i.e., $|\theta| \sim 3$–$4T_K$). The fact that the ground state of Ce in the (LaCe)Al_2 system is a doublet is confirmed by recent heat capacity measurements [34, 35] which show that the entropy associated with the Kondo heat capacity anomaly is equal to $R \ln 2$ per mole Ce. Typical results are shown in Fig. 4 for a (LaCe)Al_2 alloy with a Ce concentration of 0.64 at.-%. The low field data are well-represented by the Bloomfield-Hamann theory [36] for $S = 1/2$ and $T_K \cong 0.42$ K [in the Bloomfield-Hamann theory, $T_K \sim 3T_{max}$ where T_{max} (140 mK for this case) is the temperature at which the heat capacity anomaly attains its maximum value]. From these results, it is quite obvious that at superconducting temperatures, conduction electrons must exchange scatter from a doublet ground state which is characterized by an effective spin S_{eff} of 1/2 and that the Kondo temperature T_K is much smaller than T_{c_0}. Other characteristic anomalies occur in the Ce impurity contribution to the electrical resistivity $\Delta\varrho/n$ [17, 30, 37] and the thermoelectric power [38]. The thermoelectric power contributed by the Ce impurities is shown in Fig. 5 for various (LaCe)Al_2 alloys. The temperature dependences of both the electrical resistivity and thermoelectric power of (LaCe)Al_2 are typical of Kondo systems with low values of T_K (i.e., $T_K \ll T_{c_0}$). Finally, nuclear orientation measurements on the (LaCe)Al_2 system place T_K in the neighborhood of 0.1 K [39].

In the superconducting state, the (LaCe)Al_2 system exhibits a most unusual and striking phenomenon, that of re-entrant superconductivity where alloys with Ce impurity concentrations within a certain range exhibit two critical temperatures [40, 41]. Thus as the alloy is cooled to low temperatures, it first enters the superconducting state at a critical temperature T_{c_1} and then remains superconducting to a lower critical temperature T_{c_2} at which it then returns to the normal state for all temperatures $T < T_{c_2}$. Examples of transition curves (ac susceptibility) which exhibit a return to the normal state at a lower critical temperature and the corresponding re-entrant T_c/T_{c_0} vs *n* curve for the (LaCe)Al_2 system are shown in Figs. 6a and b [41]. In addition to the remarkable

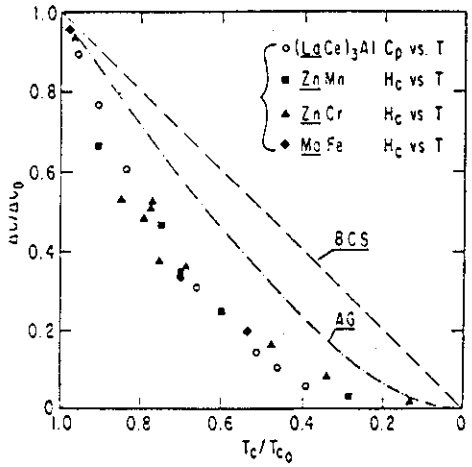

Fig. 8. Reduced specific heat jump $\Delta C/\Delta C_0$ vs reduced transition temperature T_c/T_{c_0} for the matrix-impurity systems $(LaCe)_3Al$, ZnMn, ZnCr, and MoFe. The $(LaCe)_3Al$ data (Aoi and Masuda [45]) were derived from measurements of C_p vs T and the ZnMn data (Smith [46]). ZnCr data (Vaccarone *et al.* [47]) and MoFe data (Takayanagi *et al.* [48]) were obtained from measurements of H_c vs T. The dashed line represents the BCS law of corresponding states, whereas the solid line indicates the AG result

; attributable to the formation of a bound state within the gap (band for the concentrations considered ı [34] and [35]) in the superconducting state in ontrast to the "quasi-bound state" which forms ithin the continuum of itinerant electron states in ıe normal state.

he measurements of $H_{c2}(n, T)$ show re-entrant beavior and, when analyzed within the context of the ıultiple pair breaking theory [49], yield the temperaıre dependence of the spin-flip amplitude for exıange scattering of conduction electrons by longved solute spins [37].

emperature Dependent Pair Breaking. A great deal of fort has been devoted to developing a theory for ıe superconducting properties of matrix-impurity stems which simultaneously exhibit both superonductivity and the Kondo effect. Several calculations ave shown that the superconductivity is most rongly affected when $T_K \sim T_{c_0}$. For example, it has een predicted that the initial depression of T_c with ıpurity concentration $(-dT_c/dn)_{n=0}$ will exhibit a aximum as a function of T_K/T_{c_0} near $T_K/T_{c_0} \sim 10$ 50, 51], while the initial depression of $\Delta C/\Delta C_0$ with $/T_{c_0}$, $[d(\Delta C/\Delta C_0)/d(T_c/T_{c_0})]_{T_c=T_{c_0}}$, will show a maxium as a function of T_K/T_{c_0} near $T_K/T_{c_0} \sim 1$ [52]. In a cent study of superconductivity in a series of a, Th)Ce systems, these predictions have been rified experimentally, as discussed in Section 2, which is concerned with magnetic-nonmagnetic transitions of impurities in superconductors. These predictions have strong intuitive appeal since, as previously pointed out, the relevant energy for anti-ferromagnetic pairing of conduction electron spins with impurity spins to form the so-called "quasi-bound state" is of the order of $k_B T_K$, whereas the energy for the pairing of time reversed states in a superconductor is of the order of $k_B T_{c_0}$. Other interesting properties have been predicted such as the appearance of a bound state (an impurity band for finite impurity concentrations) in the energy gap [3] and the phenomenon of re-entrant superconductivity [53, 54]. For our purposes, the most applicable and tractable of these theories is due to Müller-Hartmann and Zittartz (MHZ), and we therefore give a brief description of the theory below. The reader is referred to a recent review article by Müller-Hartmann [3] and the recent work of Schlottmann [55] for an assessment of the current status of the theory for superconducting-Kondo systems.

According to the MHZ theory, the superconducting properties in the presence of solute spins are still characterized by a pair breaking parameter α with T_c/T_{c_0} remaining the same universal function of α/α_{cr} as in the AG theory. However, for the case of $\vartheta < 0$, α must be calculated beyond order ϑ^2 which leads to the expression

$$\alpha/\alpha_{cr} = nA\left\{\frac{\pi^2 S(S+1)}{\ln^2 T/T_K + \pi^2 S(S+1)}\right\} = nA f(T/T_K), \quad (18)$$

where

$$A = 1/0.14(2\pi)^2 k_B N(E_F) T_{c_0}. \quad (19)$$

Here it should be noted that α is again *proportional to n*, but that it is now a *function of temperature*. Because of this *temperature dependent* pair breaking, α/α_{cr} cannot simply be replaced by n/n_{cr} in (10). Instead, expressions (10) and (18) must be solved simultaneously for $T_c(n)$ whose functional form depends on the ratio T_K/T_{c_0}. For $S = 1/2$ and $T_K/T_{c_0} \gtrsim 1/8$, the theory predicts that T_c is a single-valued function of n which approaches an exponential in the limit $T_K/T_{c_0} \gg 1$. For $S = 1/2$ and $T_K/T_{c_0} \lesssim 1/8$, the theory predicts the remarkable occurrence of three solutions for $T_c(n)$ in a certain impurity concentration range which depends on T_K/T_{c_0}. Thus, as the temperature is lowered, an alloy having an impurity concentration within this range should first enter the superconducting state at $T_{c1}(n)$, re-enter the normal state at $T_{c2}(n)$, and, finally, again enter the superconducting state at

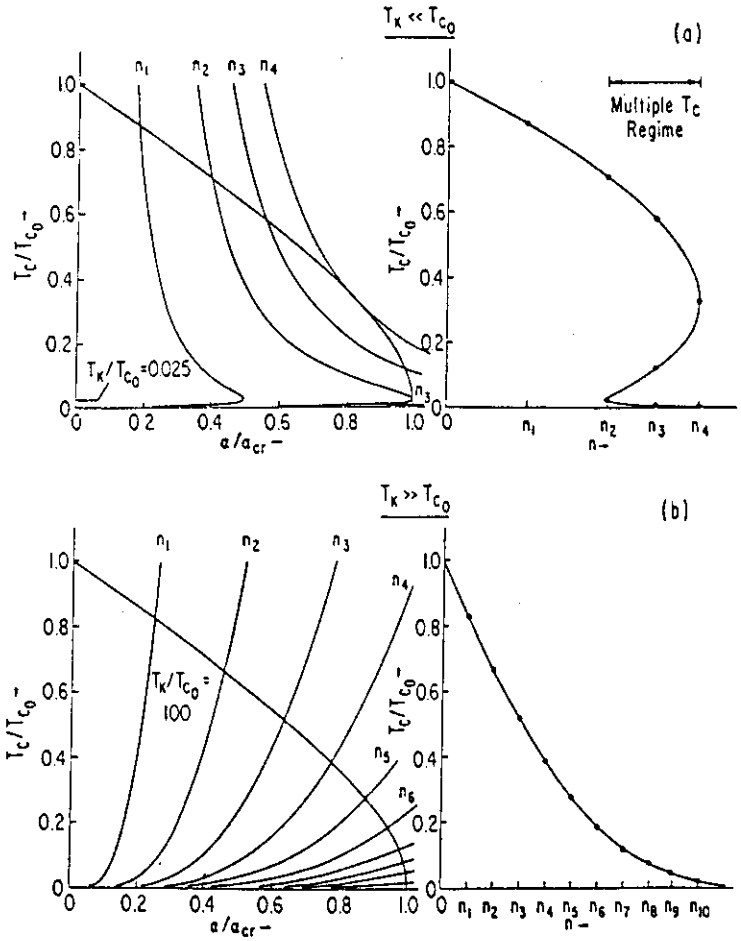

Fig. 9a and b. Illustration of the simultaneous solution of (10) and (18) to obtain the curve of T_c/T_{c_0} vs n within the context of the theory of Müller-Hartmann and Zittartz [53]. (a) Re-entrant curve of T_c/T_{c_0} vs n for $T_K/T_{c_0}=0.025$; (b) single valued relationship between T_c/T_{c_0} and n for $T_K/T_{c_0}=100$

$T_{c3}(n)$. At the boundaries of this concentration range there are two solutions for $T_c(n)$ (one of which is a turning point), and at all other concentrations, T_c is a single-valued function of n. The simultaneous solution of (10) and (18) and the corresponding behavior of T_c/T_{c_0} vs n for the cases $T_K/T_{c_0}=0.025$ and $T_K/T_{c_0}=100$ are illustrated in Figs. 9a and b.

The fact that re-entrant superconductivity has been observed in the (LaCe)Al_2 system [40, 41] and two La-rich (La, Th)Ce systems (see Section 2) is striking confirmation of the predictions of the temperature dependent pair breaking theory. For these systems, alloys within a certain concentration range were found to exhibit a return to the normal state at a critical temperature $T_{c2}(n)$ below $T_{c1}(n)$, but no evidence was found for a transition back to the superconducting state at a lower critical temperature $T_{c3}(n)$. It would therefore appear that either the third transition temperature $T_{c3}(n)$ lies below the experimental low temperature limit (6 mK in the (LaCe)Al_2 experiment [41]) or that it simply does not exist. A possible reason for the latter alternative might be that the theory does not properly take into account the *energy dependence* of the pair breaking parameter. We note, however, that a recent theory due to Schlottmann [55] also predicts for superconducting-Kondo systems in the limit $T_K \ll T_{c_0}$ that alloys within a certain impurity concentration range will exhibit a return to the normal state at a second critical temperature $T_{c2}(n)$ below $T_{c1}(n)$, but with no transition back into the superconducting state at $T_{c3}(n)$. Thus, it would be of great interest to accumulate additional evidence bearing on the existence of $T_{c3}(n)$ by means of critical field or electron tunneling measurements, for example.

Since α/α_{cr} is proportional to the rate of spin-flip exchange scattering of conduction electrons by impurity spins, it is possible, in principle, to extract the temperature dependence of the spin-flip scattering amplitude from measurements of T_c/T_{c_0} vs n by

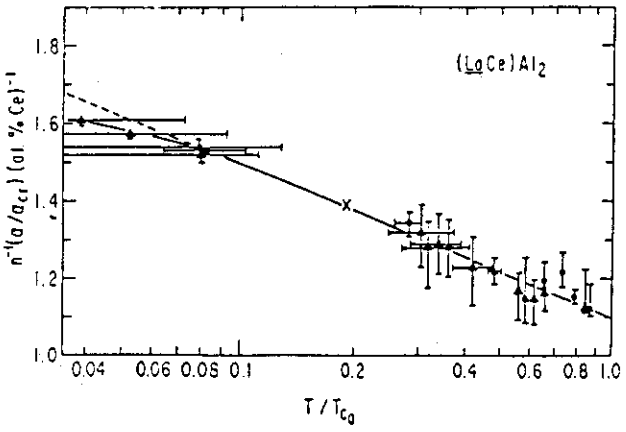

Fig. 10. Reduced pair breaking parameter $n^{-1}(\alpha/\alpha_{cr})$ vs reduced temperature T/T_{c_0} for the (LaCe)Al_2 system. The symbol (×) denotes the estimated turning point of the T_c/T_{c_0} vs n curve, while the solid circles and triangles distinguish two separately prepared sets of alloys. The dashed line is an extrapolation of the linear dependence of $n^{-1}(\alpha/\alpha_{cr})$ on $\ln T/T_{c_0}$ observed above $T/T_{c_0}=0.08$ (after Maple *et al.* [41])

inverting (10) to obtain $f(T/T_K)=(\alpha/\alpha_{cr})/nA$. This procedure has been employed [41] to obtain the temperature dependence of α/α_{cr} for the (LaCe)Al_2 system, as shown in Fig. 10. From the temperature at which $f(T/T_K)$ saturates to a constant value, we infer that $T_K \lesssim 0.1$ K, a value which is in good agreement with normal state measurements of T_K which range from ~ 0.1 K to 1 K. If the matrix happens to be a type II superconductor, in which the external field penetrates the specimen when it is in the vortex state between H_{c1} and H_{c2}, the net pair breaking parameter becomes

$$\alpha/\alpha_{cr}=nAf(T/T_K)+\frac{H_{c2}(n,T)}{H_{c2}(0,0)}=\frac{H_{c2}(0,T)}{H_{c2}(0,0)}. \qquad (20)$$

In this case, measurements of $H_{c2}(n, T)$ can be used to determine $f(T/T_K)$ by means of the relation

$$f(T/T_K)=[H_{c2}(0,T)-H_{c2}(n,T)]/nAH_{c2}(0,0). \qquad (21)$$

This procedure was first used to deduce the temperature dependence of α/α_{cr} for the LaCe system by Chaikin and Mihalisin [56] and, more recently, for the (LaCe)Al_2 system by Winzer [37]. Thus it can be seen that the temperature dependence of the spin-flip scattering amplitude, which is essentially a normal state property, can be conveniently and sensitively measured [to the extent that it is correct to relate T_c/T_{c_0} to α/α_{cr} by means of expression (10)] by studying superconducting properties such as T_c/T_{c_0} vs n and $H_{c2}(n, T)$.

With regard to the behavior of $\Delta C/\Delta C_0$ vs T_c/T_{c_0} for the (LaCe)Al_2 system, we note that the value of $[d(\Delta C/\Delta C_0)/d(T_c/T_{c_0})]_{T_c=T_{c_0}}$ yields $T_K=0.6$ K when analyzed in terms of the MHZ theory. This value is also in reasonable agreement with estimates based on normal state properties and on the curve of T_c/T_{c_0} vs n.

Finally, we comment that the recent theoretical work of Schlottmann [55] gives an excellent description of both the detailed behavior of T_c/T_{c_0} vs n and $\Delta C/\Delta C_0$ vs T_c/T_{c_0} when only one adjustable parameter, $(dT_c/dn)_{n=0}$, is fitted to the data. Also, an interesting phenomenological approach just advanced by Préjean *et al.* [57] employs the concept of a temperature-dependent effective impurity spin $S_{eff}(T)$ in conjunction with the AG theory to arrive at essentially the same result for the behavior of T_c/T_{c_0} vs n as determined by Müller-Hartmann and Zittartz.

1.3. Short-Lived Local Moments in Superconductors ($T_0 \gg T_{c_0}$)

1.3.1. Strong Itinerant-Local Electron Mixing

When the admixture of conduction electron and localized states is strong, an electron in the local state is short-lived compared to thermal fluctuation lifetimes at superconducting temperatures. The electronic structure of the local shell then loses its highly correlated atomic identity. Due to the resultant rapid temporal fluctuations of the magnetic moment associated with the localized state, the exchange interaction becomes inoperative as a mechanism by means of which the conduction electrons interact with the localized impurity states. Instead, the dominant effect on superconductivity seems to be through the strong Coulomb repulsion which two members of a Cooper pair experience when they scatter into the large local density of states at each impurity site. This Coulomb resulsion weakens the pairing due to the electron-phonon interaction so that the net attractive interaction is decreased.

Matrix-impurity systems of this type exhibit weakly magnetic behavior and various normal state anomalies that resemble those which are associated with the Kondo effect. The weakly magnetic behavior arises from the local moment fluctuations of frequency τ_{sf} with which there is a corresponding characteristic temperature $T_0=\hbar/k_B\tau_{sf}$. At temperatures much greater than T_0, thermal fluctuation lifetimes are much smaller than τ_{sf} and the magnetic susceptibility follows a Curie-Weiss law, (8), where the Curie-Weiss

temperature θ is independent of concentration and of the order of $-(3\text{–}4)\,T_0$. However, for temperatures much smaller than T_0, the thermal fluctuation lifetimes are long compared to τ_{sf} so that the resultant magnetic moment averages over time to zero and the susceptibility approaches a constant value in the limit $T\to 0$. The types of impurity which belong to this category include transition metal, rare earth and actinide impurities, depending, again, on the electronic structure of the matrix into which the impurities have been imbedded. As an exemplary matrix-impurity system, we consider the ThU system.

Exemplary System—ThU. The anomalies which occur in the normal state physical properties of the ThU system indicate that the characteristic local moment fluctuation temperature T_0 is of the order of 100 K, much larger than the transition temperature of the matrix ($T_{c_0} = 1.4$ K). First, the magnetic susceptibility follows a Curie-Weiss law for $T \gtrsim 100$ K with an effective magnetic moment $\mu_{eff} = 3.4\mu_B$, a value which is close to that expected for either 2 or 3 electrons in the U $5f$ shell, and a negative Curie-Weiss temperature $-\theta \sim 290\text{ K} \sim 3T_0$ [58]. For $T \lesssim 100$ K, the susceptibility departs somewhat from the Curie-Weiss law, approaching a finite value in the limit $T\to 0$ [58]. The ThU magnetic susceptibility as a function of temperature is shown in Fig. 11. Second, the electrical resistivity exhibits a minimum at low temperatures and the incremental resistivity contributed by the U ions varies as $[1-(T/T_0)^2]$ with $T_0 \sim 100$ K [58]. This is illustrated in Fig. 12. Third, there is a giant positive peak in the thermoelectric power at ~ 80 K (Fig. 13), again suggesting a characteristic temperature $T_0 \sim 100$ K [58]. Finally, the enhancement of the electronic specific heat coefficient γ is quite large, equivalent to a local U density of states at the Fermi level of ~ 70 states/eV-U atom at low U concentrations [59, 60].

In the superconducting state, the T_c/T_{c_0} vs n curve for the ThU system exhibits pronounced positive curvature [58] as shown in Fig. 14. This is in stark contrast to the negative curvature of the T_c/T_{c_0} vs n curves for the two long-lived local moment regimes discussed in Subsections 1.1 and 1.2. Another interesting point is that the initial depression of T_c, $(-dT_c/dn)_{n=0}$, is equal to 8 K/at.-% U for the ThU system [58]. This value is much larger than the 3 K/at.-% Gd exhibited by the ThGd system [23, 61] in which the Gd ions have long-lived magnetic moments ($\mu_{eff} \sim 8\mu_B$), a large total angular momentum ($J = S = 7/2$), and a positive exchange interaction parameter ($\theta > 0$). Thus it is

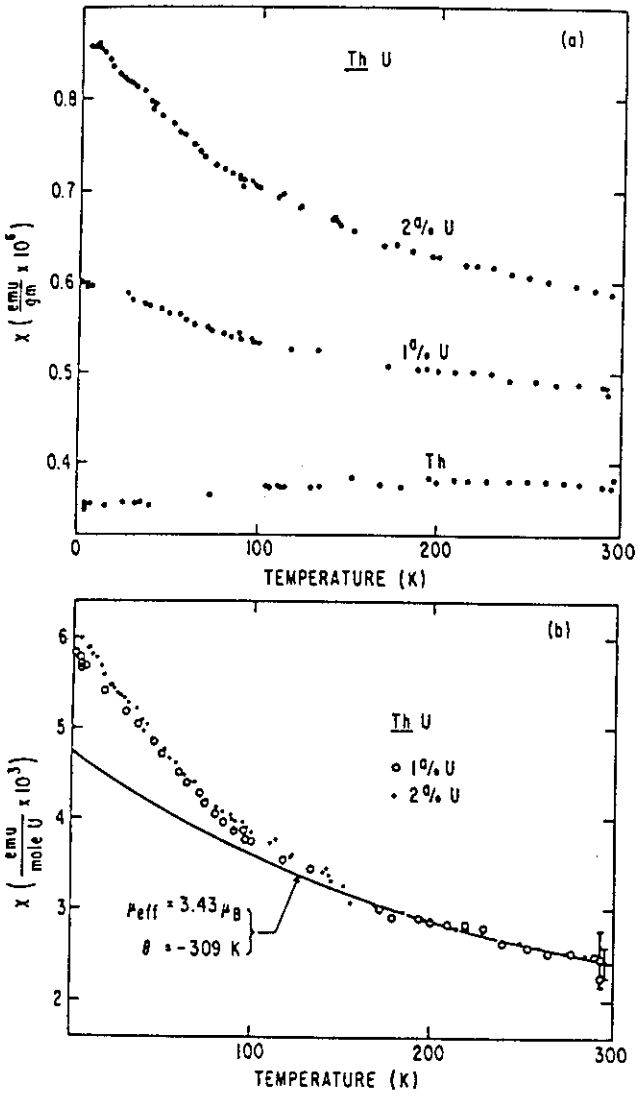

Fig. 11. (a) Magnetic susceptibility of pure Th and ThU alloys as a function of temperature. (b) Magnetic susceptibility (corrected for the Th background susceptibility) of ThU alloys vs temperature. The solid line represents a Curie-Weiss law for an effective moment of 3.43 Bohr magnetons and a Curie-Weiss temperature $\theta = -309$ K (after Maple *et al.* [58])

apparent that a large value of $(-dT_c/dn)_{n=0}$ cannot, as once presumed, be taken as evidence for the existence of a "magnetic" impurity since the magnetic susceptibility of the ThU system shows that it is a very weakly magnetic system compared to ThGd. This emphasizes the point that the magnetic state of an impurity cannot be determined from measurements of $-(dT_c/dn)_{n=0}$ only—this requires additional measurements of the detailed dependence of T_c/T_{c_0} vs n and

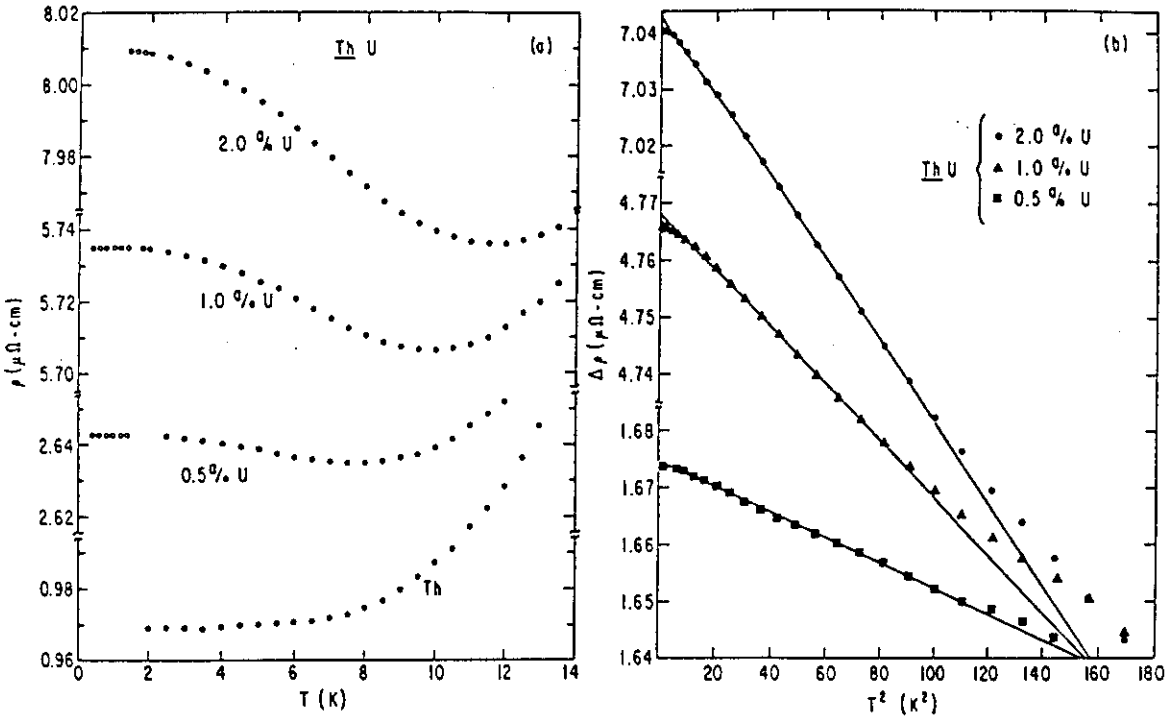

Fig. 12. (a) Electrical resistivity of Th and ThU alloys vs temperature. (b) Incremental resistivity ($\Delta\varrho \equiv \varrho - \varrho_{Th}$) of ThU alloys vs temperature squared (after Maple *et al.* [58])

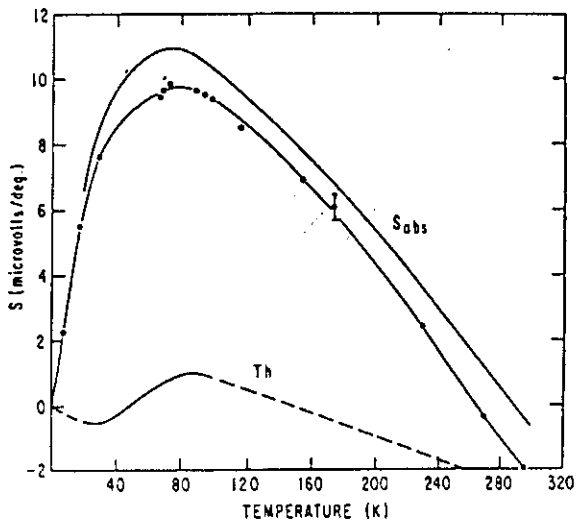

Fig. 13. Thermoelectric power of a ThU alloy (3 at.-% U) with respect to copper. The curve marked S_{abs} is the corresponding temperature dependence of the *absolute* thermoelectric power of the alloy (after Maple *et al.* [58])

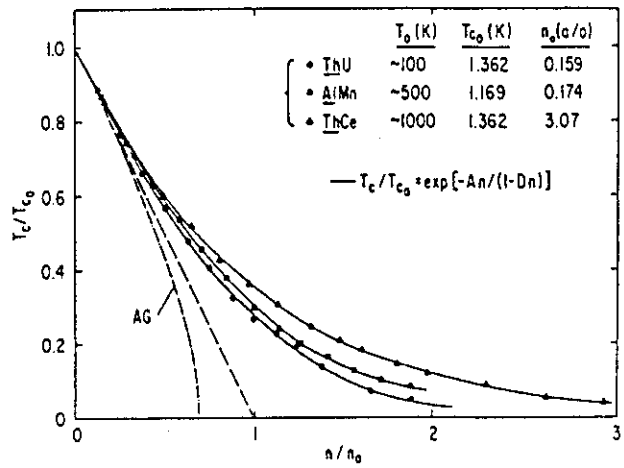

Fig. 14. Reduced transition temperature T_c/T_{c_0} vs reduced concentration n/n_0 for the system ThU [58], AlMn [62] and ThCe [14]. The values of n_0 were chosen to normalize the initial slope $[d(T_c/T_{c_0})/d(n/n_0)]_{n=0}$ to the value -1. The solid lines are modified exponential relations of the form proposed by Kaiser [63] which have been fitted to the data by the method of least squares

of $\Delta C/\Delta C_0$ vs T_c/T_{c_0}. Also shown in Fig. 14 are T_c/T_{c_0} vs n curves for the related systems AlMn [62] and ThCe [13, 14] which exhibit pronounced positive curvature like the ThU system. These systems too are weakly magnetic with $T_0 \gg T_{c_0}$. All three curves in Fig. 12 have been fitted by a modified exponential function

$$T_c/T_{c_0} = \exp[-An/(1-Dn)] \qquad (22)$$

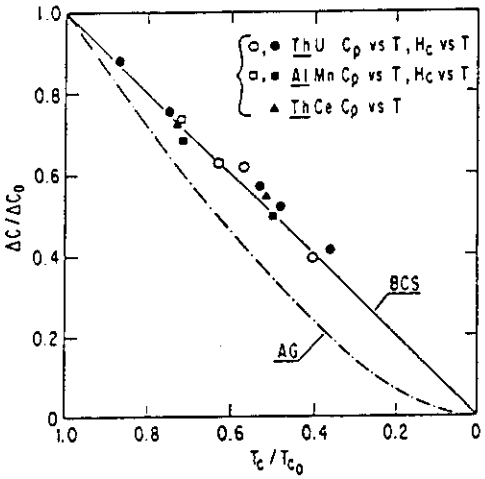

Fig. 15. Reduced specific heat jump $\Delta C/\Delta C_0$ vs reduced transition temperature T_c/T_{c_0} for the ThU, AlMn and ThCe systems. The solid line represents the BCS law of corresponding states, whereas the dot-dashed line indicates the AG result. Open circles—data from Luengo *et al.* [59, 60]; solid circles—data from Watson *et al.* [64]; open square—data from Martin [66]; solid squares—data from Smith [65]; solid triangles—data from Dempesy [67]

first proposed by Kaiser [63], which is indicated by the solid lines in the figure.

The basic nonmagnetic nature of the matrix-impurity systems for which $T_0 \gg T_{c_0}$ is clearly reflected in the behavior of their curves of $\Delta C/\Delta C_0$ vs T_c/T_{c_0}. This is shown in Fig. 15 for the exemplary ThU system [59, 60, 64] and for the AlMn [65, 66] and ThCe [67] systems as well. For all three systems, the reduced specific heat jump follows the BCS law of corresponding states $\Delta C/\Delta C_0 = T_c/T_{c_0}$. The data plotted in Fig. 15 have been derived both from specific heat and critical field measurements. In the latter case, the specific heat jumps have been extracted with the aid of Rutger's relation (9). We remark that the behavior of H_c vs T for both the ThU [64] and AlMn [65] systems follows closely the BCS behavior.

Pair Weakening. The general features of the superconducting properties of matrix-impurity systems for which $T_0 \gg T_{c_0}$ can be accounted for by a model in which the impurities contribute localized d or f states which are non-magnetic in the sense of the Friedel-Anderson model (i.e., $\pi\Delta/U > 1$). This model has been developed through a series of papers by Zuckermann [68], Ratto and Blandin [69], Takanaka and Takano [70], and, most recently, by Kaiser [63]. Kaiser's formulation is of particular interest since he was the first to calculate the full impurity concentration dependence of T_c from the Ratto-Blandin Hamiltonian (the BCS Hamiltonian in conjunction with the nonmagnetic Anderson Hamiltonian).

According to Kaiser's theory, $T_c(n)$ is given by a modified exponential relation of the form represented by (22) with the parameters A and D given by

$$A = (2L+1)\frac{N_l(E_F)}{N(E_F)}\left[1 + \frac{N_l(E_F)U_{\text{eff}}}{N(E_F)V}\right] \Big/ N(E_F)V \tag{23}$$

and

$$D = \frac{N_l(E_F)}{N(E_F)}\,\frac{(2L+1)N_l(E_F)U_{\text{eff}}}{N(E_F)V}. \tag{24}$$

Here, $N_l(E_F)$ is the local density of states at an impurity site (without spin and orbital degeneracy), V is the electron-phonon interaction parameter, U_{eff} is the intra-atomic Coulomb repulsion which splits spin-up and spin-down states in the Friedel-Anderson model (reduced by correlations [71]), and L is the orbital quantum number. In terms of the Hartree-Fock parameters (Δ, E_l, and U), $N_l(E_F)$ is given by (2) where

$$E_l = \Delta \cot\left[\frac{\pi\langle N\rangle}{2(2L+1)}\right] \tag{25}$$

and $\langle N\rangle$ is the local state occupation number, while

$$U_{\text{eff}} = \frac{U}{1 + (U/\pi E_l)\tan^{-1}(E_l/\Delta)}. \tag{26}$$

Physically, the modified exponential depression of T_c with n which emerges from Kaiser's calculation arises from two ways in which the presence of the nonmagnetic impurity resonant states weakens the pairing of superconducting electrons in the matrix via the electron-phonon interaction. The first is a one-body dilution effect that reduces the density of states, while the second is a two body effect which decreases the coupling constant $N(E_F)V$ by virtue of strong Coulomb repulsion between two members of a Cooper pair $(k\uparrow, -k\downarrow)$ after they have scattered into the local state. In fact, these two effects can be identified by casting (22) in the form of a BCS equation

$$T_c = 1.14\theta_D \exp(-1/g') \tag{27}$$

with an "effective" coupling constant g' which is given by

$$g' = g\,\frac{1 - Dn}{1 + (Ag - D)n}, \tag{28}$$

where $g = N(E_F)V$ is the BCS coupling constant for the matrix. By substituting expressions (23) and (24)

for the parameters A and D into (28), it can easily be shown that

$$g' = N(E_F)V \frac{N(E_F)}{N(E_F)+n(2L+1)N_l(E_F)} - N_l(E_F)U_{eff} \frac{n(2L+1)N_l(E_F)}{N(E_F)+n(2L+1)N_l(E_F)}. \quad (29)$$

The first term, which represents the one body dilution effect considered by Zuckermann, reveals how the density of states $N(E_F)$ is reduced by the phase-space factor

$$f = \frac{N(E_F)}{N(E_F)+n(2L+1)N_l(E_F)} \quad (30)$$

representing the probability of finding an electron in the conduction band. The second term, which is associated with the two body Coulomb repulsion effect first treated by Ratto and Blandin, and Takanaka and Takano, shows how the coupling constant is reduced by the intra-atomic Coulomb repulsion factor $N_l(E_F)U$ weighted by the phase-space factor

$$1-f = \frac{n(2L+1)N_l(E_F)}{N(E_F)+n(2L+1)N_l(E_F)} \quad (31)$$

which represents the probability of finding an electron in the localized state. It should also be noted that (22) implies that there is a critical concentration n_{cr} at which $T_c' \to 0$ which is given by

$$n_{cr} = D^{-1} = \frac{N(E_F)}{N_l(E_F)} \frac{N(E_F)V}{(2L+1)N_l(E_F)U_{eff}}. \quad (32)$$

Since the interaction between the conduction electrons and the impurities is essentially of nonmagnetic nature (the Ratto and Blandin Hamiltonian preserves time reversal symmetry), the calculation by Kaiser predicts that the thermodynamic properties such as $\Delta C/\Delta C_0$ vs T_c/T_{c_0} follow the BCS law of corresponding states.

Although the nonmagnetic resonant state model does not take into account the impurity spin dynamics which are implicit in the concept of a temporally fluctuating solute spin, it describes the T_c/T_{c_0} vs n and $\Delta C/\Delta C_0$ vs T_c/T_{c_0} curves for a number of matrix-impurity systems with $T_0 \gg T_{c_0}$ remarkably well. It is significant that recent theories which take into account the existence of localized spin fluctuations give essentially the same results as long as $T_0 \gg T_{c_0}$ ("fast" localized spin fluctuations) [72].

Finally, Fig. 16 depicts schematically the systematics of superconductivity in the presence of local moments

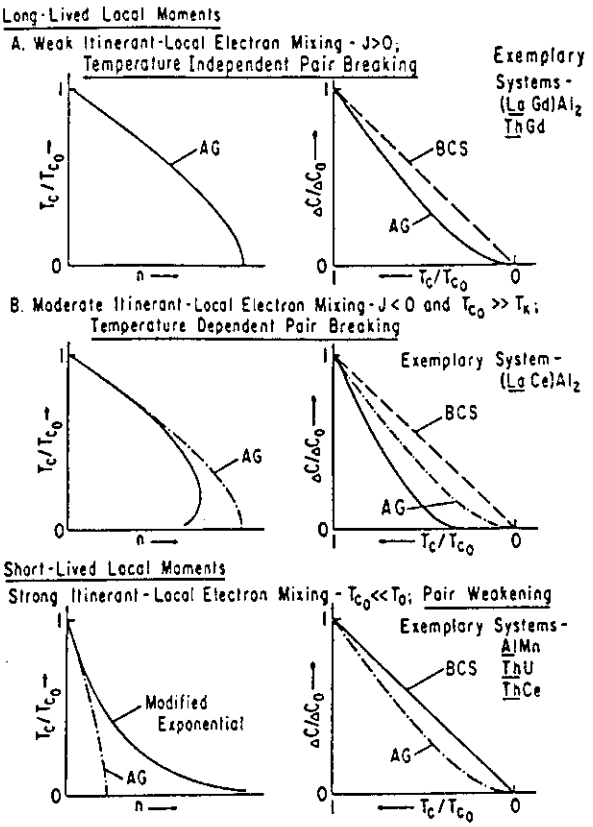

Fig. 16. The systematics of superconductivity in the presence of local moments. The solid lines represent the behavior of the curves of T_c/T_{c_0} vs n and $\Delta C/\Delta C_0$ vs T_c/T_{c_0} for each of the three regimes of solute magnetic behavior

for the three distinct regimes of solute magnetic character which have been identified. It is quite evident that these three regimes can be distinguished clearly by the *detailed* variations of T_c/T_{c_0} with n and $\Delta C/\Delta C_0$ with T_c/T_{c_0}.

2. Magnetic-Nonmagnetic Transitions of Impurities in Superconductors

In certain matrix-rare earth impurity systems, a continuous demagnetization of the rare earth impurities can be induced by applying an external pressure or by varying the composition of the matrix if it is a binary alloy. Apparently, this increases the extent to which the itinerant electrons admix with localized electrons so that the solute spin lifetime passes from the long-lived to the short-lived regimes. Such magnetic-nonmagnetic transitions are dramatically reflected in the superconducting properties

which evolve from pair breaking to pair weakening behavior as the solute magnetic moment lifetime passes from long-lived to short-lived. We consider two exemplary matrix-impurity systems, LaCe and (La, Th)Ce. In the former system, a continuous demagnetization of the Ce impurities can be induced by applying an external pressure, whereas in the latter system it can be generated by increasing the Th composition of the La, Th binary alloy matrix.

2.1. Continuous Demagnetization of Impurities in Superconductors Induced by an External Pressure

Pressure-induced magnetic-nonmagnetic transitions of a rare earth impurity in a metallic matrix were first reported for the superconducting matrix-impurity systems $(LaCe)_3In$ [73] and LaCe [74]. The transition was inferred from the pronounced features in the variation of the superconducting transition temperature T_c with pressure. The most extensive studies were made on the LaCe system, the results of which are discussed below.

2.1.1. Exemplary System—LaCe Under Pressure

At zero pressure, Ce impurities in an fcc La matrix are trivalent and support long-lived local moments as indicated by the behavior of the magnetic susceptibility as a function of temperature. Similar to the $(LaCe)Al_2$ system, the temperature dependence of the susceptibility further suggests that the cubic crystal field of the La matrix splits the Ce^{3+} $J=5/2$ Hund's rule multiplet into a ground state doublet and an excited state quartet with a splitting $\delta \sim 10^2$ K [2, 75]. Thus at superconducting temperatures, a doublet ground state with an effective spin $S_{eff}=1/2$ is again responsible for conduction electron exchange scattering. From the behavior of the low temperature electrical resistivity ϱ and other properties as well [76], it can be inferred that the conduction electron-impurity spin exchange coupling is antiferromagnetic ($\vartheta<0$) and that the Kondo temperature T_K is low—much smaller than the critical temperature $T_{c_0}=6.0$ K of the La host. In the range of Ce impurity concentration where interaction effects are negligible, the superconducting properties can be rather well accounted for by *temperature dependent pair breaking* theories such as the one formulated by MHZ.

The primary superconductivity data documenting the pressure-induced demagnetization of Ce impurities in the LaCe system [74] are displayed in Fig. 17. With increasing Ce concentration, a minimum in T_c as a function of pressure P develops near 15 kbar which becomes more pronounced the higher the Ce concentration. The initial depression of T_c, $\Delta T_c/n$, markedly increases with pressure up to a maximum near 15 kbar and thereafter decreases to a value which, above ~ 100 kbar, is more than an order of magnitude smaller than the maximum depression. Isobars of T_c as a function of n in the inset of Fig. 17 show that the shape of the T_c vs n curve evolves with increasing pressure from nearly linear depressions with slight negative curvature to depressions with strong positive curvature. This latter behavior is very similar to the *nonmagnetic* ThCe system for which T_c exhibits a modified exponential decrease with n at zero pressure [14]. Thus, from the evolution of the T_c/T_{c_0} vs n curves as a function of pressure, it has been inferred that

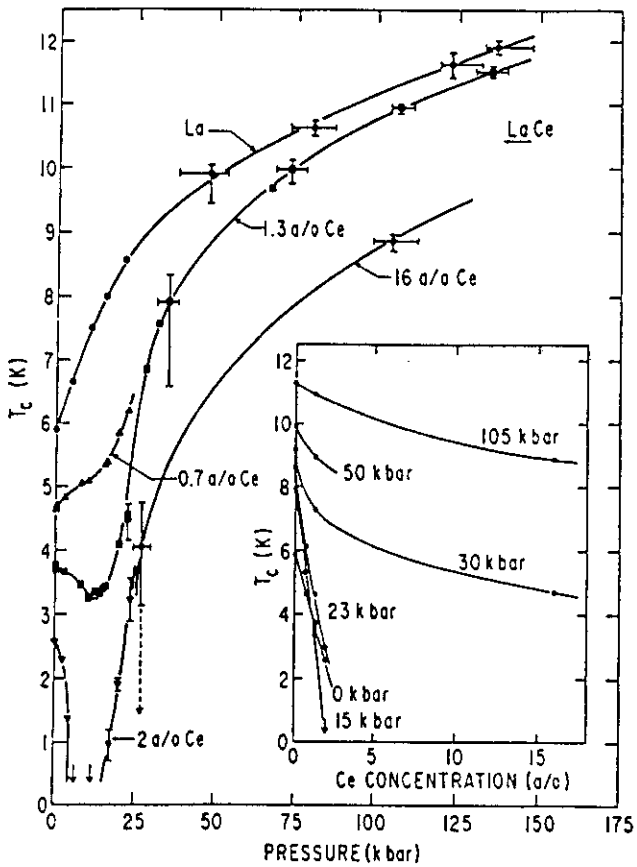

Fig. 17. Pressure dependence of the superconducting transition temperature T_c of as-cast predominantly fcc La and LaCe alloys to very high pressure. The vertical bars represent the transition widths and the horizontal bars the pressure inhomogeneity in the high-pressure cell. Isobars of T_c vs Ce concentration are shown in the inset (after Maple *et al.* [74])

Ce impurities in La experience a pressure-induced continuous demagnetization as the solute moment passes from long-lived to short-lived. The normal state electrical resistivity of LaCe alloys has also been studied as a function of pressure to 18 kbar [77]. The slope $|d(\Delta\varrho)/d\ln T|$ in the range of temperatures where the Ce contribution $\Delta\varrho$ to the resistivity is linear in $\ln T$ was also found to exhibit a maximum near 15 kbar.

The existence of the pronounced maximum in the initial depression of T_c, $(-dT_c/dn)_{n=0}$, follows from the fact that the magnitude of the exchange interaction parameter $|\mathcal{J}|$, and in turn the Kondo temperature $T_K \sim T_F \exp[-1/N(E_F)|\mathcal{J}|]$, initially increases with pressure. Since the zero pressure value of T_K/T_{c_0} is only $\lesssim 0.2$, an increase of T_K/T_{c_0} with pressure implies a corresponding increase in $(-dT_c/dn)_{n=0}$, according to the calculations of MHZ [51] which show that $(-dT_c/dn)_{n=0}$ increases with T_K/T_{c_0} until it reaches a maximum at $T_K/T_{c_0} \sim 10$. From the inferred increase of $|\mathcal{J}|$ with pressure, one can see from expression (16) that this could be caused by a decrease of the energy E_l separating the Ce resonant state and the Fermi level or an increase of the matrix element V_{kl} [or, equivalenty, the Hartree-Fock half-width of the resonant state $\Delta = \pi\langle V_{kl}^2\rangle N(E_F)$] with pressure (the intra-atomic Coulomb repulsion U is expected to remain nearly constant). However, both a decrease of E_l or an increase of V_{kl} have the effect of driving the magnetic moment more unstable; or, in other words, decreasing the local moment lifetime. If the local moment lifetime is decreased too much, then the appropriateness of the exchange interaction Hamiltonian and any conclusions which are based on it become doubtful. Thus, the central question is at what pressure does the exchange model become an inadequate description of the manner in which the solutes interact with the conduction electrons and, in turn, affect the superconductivity of the matrix. Considerable controversy has, in fact, raged over just this point. One school of thought [74, 78] has favored the pressure-induced demagnetization of the Ce ions, with the decrease in the initial depression of T_c and the exponential like depression of T_c with n at high pressures as evidence for the existence of short-lived local moments as in the ThCe system at zero pressure (which is known to be nonmagnetic from the adherence of the $\Delta C/\Delta C_0$ vs T_c/T_{c_0} curve to the BCS law of corresponding states). The decrease of the lifetime of the local moment is here believed to be associated with the passage of the Ce $4f$ level through the Fermi level of the matrix as a function of pressure. On the other hand, the rival school of thought [51, 79] attributes the same decrease of the initial depression of T_c (after the maximum) and the exponential like dependence of T_c on n at high pressure as evidence for a large value of the Kondo temperature ($T_K \gg T_{c_0}$). Both features would follow quite naturally from the MHZ theory if it is assumed that the Ce moments remain long-lived and that $|\mathcal{J}|$ (and, in turn, T_K) increases monotonically with pressure up to the highest pressures attained which were ~ 140 kbar. Thus the Ce $4f$ level always remains below E_F and the effects are due to the passage of the characteristic temperature T_K for the formation of the quasibound state through T_{c_0} and culminating in the state where $T_K \gg T_{c_0}$ at which the *matrix-impurity* system can be regarded as nonmagnetic.

One interesting way to distinguish between these two alternatives is to measure the initial depression of the reduced specific heat jump $\Delta C/\Delta C_0$ with reduced transition temperature T_c/T_{c_0} for the LaCe system as a function of pressure. In the first case where the Ce moments are presumed to be short-lived ($T_0 \gg T_{c_0}$) at high pressure, the quantity $[d(\Delta C/\Delta C_0)/d(T_c/T_{c_0})]_{T_c=T_{c_0}}$ is expected to converge to 1 (the BCS value) with increasing pressure. In the second case where the Ce moments are presumed to be long-lived ($T_0 \ll T_{c_0}$) at high pressure, the quantity $[d(\Delta C/\Delta C_0)/d(T_c/T_{c_0})]_{T_c=T_{c_0}}$ is expected to approach 1.43 (the AG value) with increasing pressure since the MHZ theory predicts that the initial depression of the reduced specific heat jump with reduced transition temperature equals 1.43 in the limit $T_K/T_{c_0} \to \infty$. Unfortunately, experimental difficulties attendant to heat capacity measurements at very high pressure have thus far prevented the acquisition of these data with which this question could be answered. On the other hand, the magnetic-nonmagnetic transition of Ce impurities in La which is induced by the application of pressure can also be induced by alloying the La matrix with Th. This offers the possibility of collecting extensive data for both T_c/T_{c_0} vs n and $\Delta C/\Delta C_0$ vs T_c/T_{c_0} with which to document the Ce demagnetization in the (La, Th)Ce system in detail while it proceeds as the Th composition of the La, Th binary alloy matrix is increased.

It should also be remarked here that a pressure-induced magnetic-nonmagnetic transition also occurs in the YCe system [80, 81]. However, the superconductivity of this system can only be studied at pressures in excess of 100 kbar where the Ce moments

are already short-lived compared to thermal fluctuations at the superconducting temperatures of interest.

2.2. Continuous Demagnetization of Impurities in Superconductors Induced by Variation of the Composition of a Binary Alloy Matrix

There have been a number of superconductivity experiments in which the composition of a binary alloy solvent has been varied to induce changes in the magnetic character of a solute. The systems which have been studied include (Zn, Al)Mn [82], (Y, Th)Ce [83], (La, Y)Ce [84], and (La, Th)Ce [85–88]. We have chosen to discuss the properties of the latter system since it offers the greatest range of solute magnetic character over which the superconducting properties can be studied and it has been more extensively investigated than any of the other systems.

2.2.1. Exemplary System—(La, Th)Ce

A magnetic-nonmagnetic transition of Ce impurities which proceeds with increasing Th composition in the (La, Th)Ce system appears to be the analogue of the transition induced by pressure in the LaCe system. This is suggested by recent measurements which show that the initial depression of T_c with Ce concentration, $(-dT_c/dn)_{n=0}$, displays a pronounced maximum as a function of Th concentration similar to that which occurs as a function of pressure in the LaCe system [85, 86]. The depth of the maximum and the decrease of the lattice parameter at which it occurs are nearly the same in the (La, Th)Ce system as in the LaCe system under pressure [85]. Thus the (La, Th)Ce system affords a unique opportunity for studying in detail the evolution of the superconducting and normal state properties of a matrix-impurity system as the impurity demagnetization proceeds; that is, as the solute spin lifetime passes from long-lived to short-lived compared to thermal fluctuation lifetimes at superconducting temperatures. In particular, detailed curves of T_c/T_{c_0} vs n and $\Delta C/\Delta C_0$ vs T_c/T_{c_0} may be conveniently mapped out at zero pressure. The only drawback to studying magnetic-nonmagnetic transitions of impurities which are induced by varying the composition of a binary alloy matrix is associated with the statistical distribution of matrix metal atoms which surround an impurity and the complications

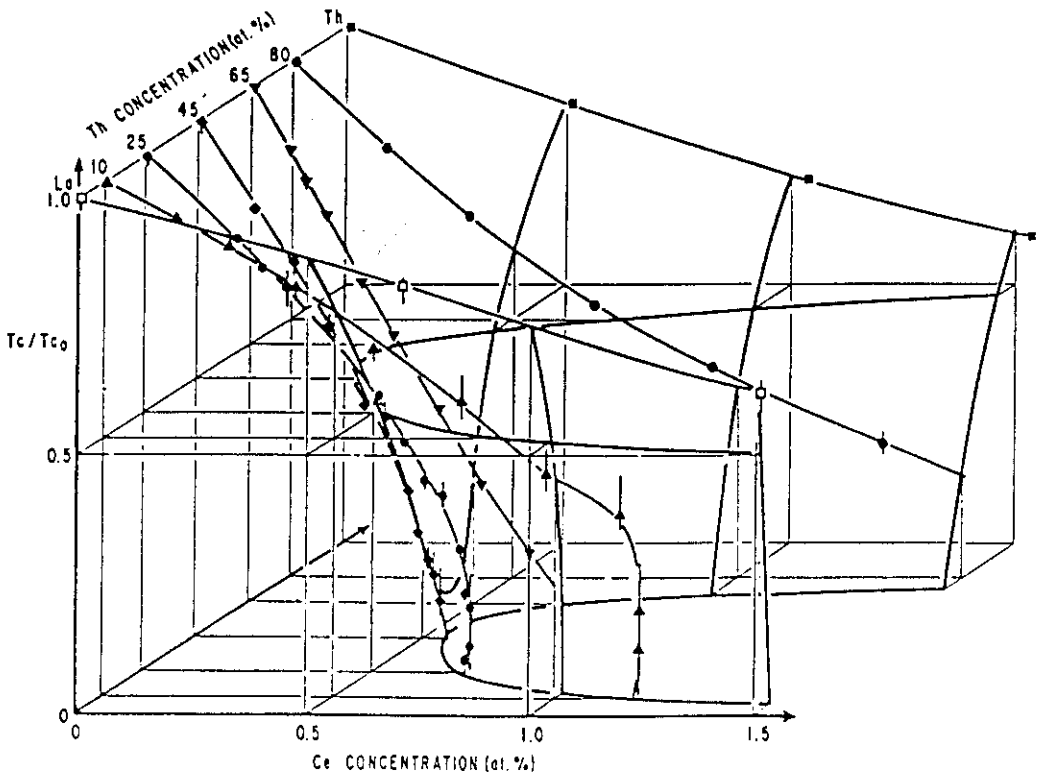

Fig. 18. Normalized transition temperature T_c/T_{c_0} vs Ce concentration and Th concentration for (La, Th)Ce. The curves of T_c/T_{c_0} vs Ce concentration for the $La_{0.90}Th_{0.10}Ce$ and the $La_{0.75}Th_{0.25}Ce$ systems are re-entrant (after Huber *et al.* [86])

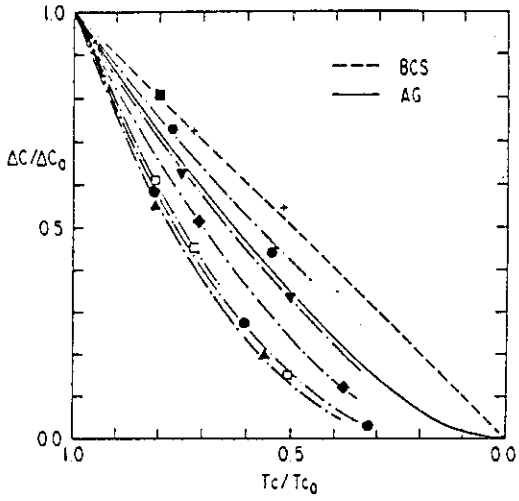

Fig. 19. Reduced specific heat jump $\Delta C/\Delta C_0$ vs reduced critical temperature T_c/T_{c_0} for (La, Th)Ce. Open squares, LaCe; upright triangles, $La_{0.90}Th_{0.10}Ce$; circles, $La_{0.75}Th_{0.25}Ce$; diamonds, $La_{0.55}Th_{0.45}Ce$; inverted triangles, $La_{0.35}Th_{0.65}Ce$; hexagons, $La_{0.20}Th_{0.80}Ce$; solid square and crosses, ThCe (after Luengo *et al.* [87, 88])

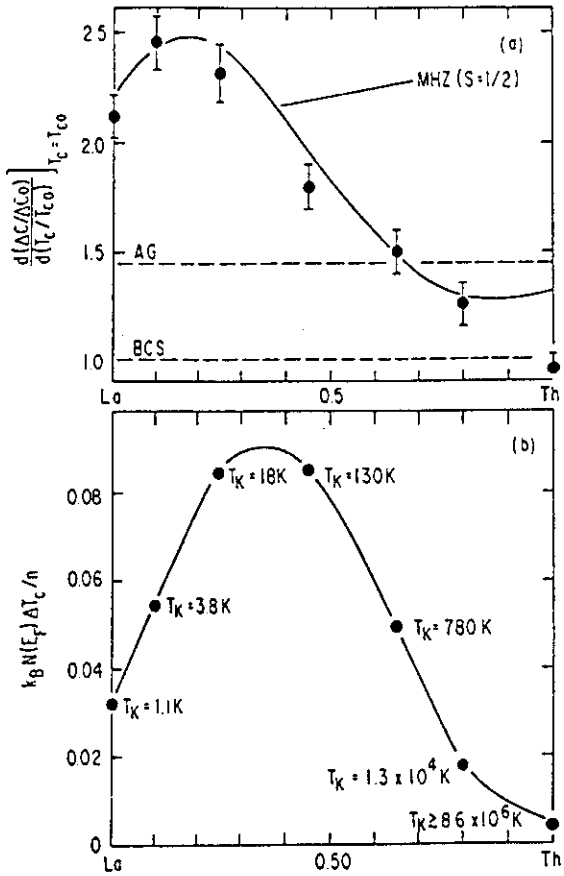

Fig. 20. (a) Initial slope $[d(\Delta C/\Delta C_0)/d(T_c/T_{c_0})]_{T_c=T_{c_0}}$ vs Th composition for the system (La, Th)Ce. The solid line was derived from the MHZ theory [52] using the data for $k_B N(E_F)\Delta T_c/n$. (b) The quantity $k_B N(E_F)\Delta T_c/n$ vs Th composition for the system (La, Th)Ce. The Kondo temperatures T_K were obtained by fitting the data with the MHZ calculation (after Luengo *et al.* [87, 88])

incurred thereof [89]. Fortunately, this factor does not appear to present a serious problem in interpreting the results of the investigations on the (La, Th)Ce system.

Detailed measurements of T_c/T_{c_0} vs n [86] and $\Delta C/\Delta C_0$ vs T_c/T_{c_0} [87, 88] have been made for the (La, Th)Ce system in two recent studies. The resulting T_c/T_{c_0} vs n curves are shown in Fig. 18 for several different values of La, Th matrix composition. Displayed in this three-dimensional plot are all the variations which are found in the T_c/T_{c_0} vs n curves across the continuum from LaCe to ThCe; the pronounced maximum in the initial depression of T_c vs n, the smooth sweep from negative to positive curvature, and the appearance of re-entrant superconductivity. The curves obtained for $\Delta C/\Delta C_0$ vs T_c/T_{c_0} are shown in Fig. 19. With the exception of pure Th, all La, Th compositions studied yielded $\Delta C/\Delta C_0$ vs T_c/T_{c_0} curves which deviated from the BCS law of corresponding states. Similar to the initial depression of T_c with n which exhibits a maximum at a La, Th host composition ~45 at.-% Th, the initial depression of $\Delta C/\Delta C_0$ with T_c/T_{c_0} sweeps through a maximum at a La, Th host composition of ~15 at.-% Th. Thus the data of Figs. 18 and 19 document in detail the evolution of T_c/T_{c_0} vs n and $\Delta C/\Delta C_0$ vs T_c/T_{c_0} when an impurity in a superconducting matrix-impurity system undergoes a magnetic-nonmagnetic transition; or, equivalently, when the impurity moment passes from long-lived to short-lived compared to thermal fluctuation lifetimes at superconducting temperatures.

The data of Figs. 18 and 19 also provide a means of determining the range of Th concentrations over which the Ce moments remain longlived and, apparently, the exchange model an adequate description of the manner in which the impurity moments affect superconducting electron pairs. This involves a self-consistent analysis of the data which incorporates the temperature dependent pair breaking theory of MHZ. The analysis was carried out in the following manner. First, the maximum in the experimental curve of the quantity $k_B N(E_F)\Delta T_c/n$ [$N(E_F)$ is the bare density of states at the Fermi level] vs Th concentration shown

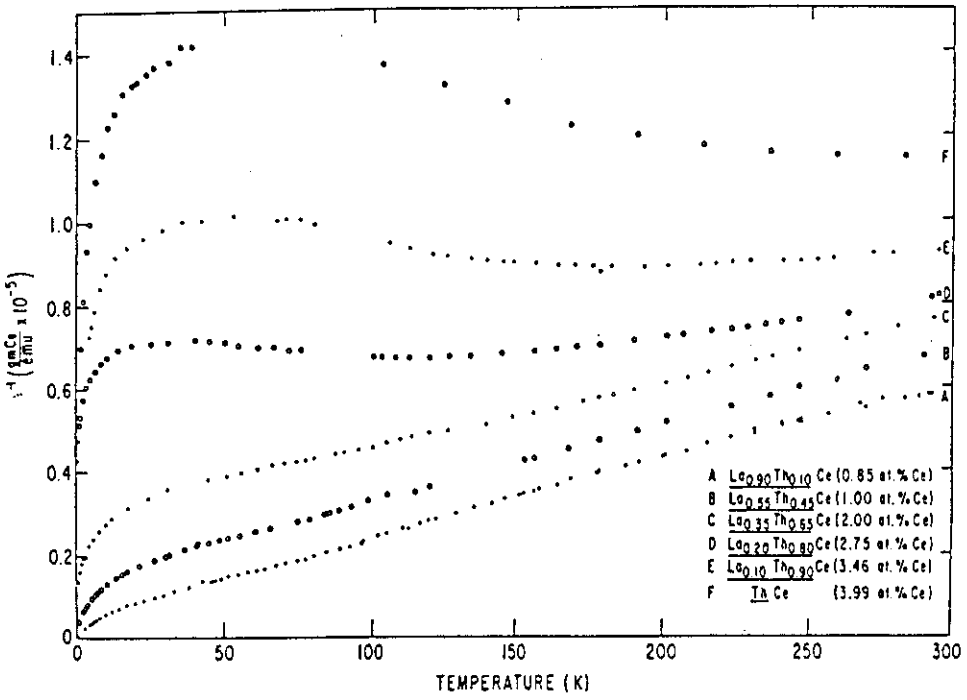

Fig. 21. Inverse magnetic susceptibility vs temperature for (La, Th)Ce alloys with La, Th matrix compositions of 10, 45, 65, 80, 90, and 100 at.-% Th (after Huber *et al.* [91])

in Fig. 20b was scaled to the maximum in the theoretical MHZ curve of $k_B N(E_F)\Delta T_c/n$ vs T_K/T_{c0}. Values of T_K indicated in Fig. 20b were obtained by matching the experimental points to the MHZ curve and then used to construct the theoretical MHZ curve for $[d(\Delta C/\Delta C_0)/d(T_c/T_{c0})]_{T_c=T_{c_0}}$ vs Th composition in Fig. 20a (without scaling). It can be seen that the MHZ theory and the specific heat data are in good agreement to Th concentrations ~70 at.-%, but they definitely diverge at higher Th concentrations—the MHZ theoretical curve approaching the value given by the temperature independent pair breaking theory of AG in the limit $T_K/T_{c0} \to \infty$, and the experimental data converging to the BCS value realized at 100 at.-% Th. Although the maximum in both the theoretical and experimental curves near 15 at.-% Th is especially striking, it should be pointed out that the agreement to such high Th concentrations may be somewhat fortuitous since the superconducting properties during the magnetic-nonmagnetic transition must go smoothly from pair breaking to pair weakening behavior as the solute spin lifetime passes from long-lived to short-lived. Clearly, a theory is needed which takes into consideration the variation of the solute spin lifetime and reduces to the MHZ theory in the long-lived (magnetic) limit and to a theory, such as the one due to Kaiser, in the short-lived (nonmagnetic) limit. The experiments reviewed here lay the foundation for such a theory and emphasize the necessity of taking into consideration the solute spin lifetime.

In addition to the aforementioned superconducting properties, the normal state electrical resistivity [90] and magnetic susceptibility [91] of the (La, Th)Ce system have been measured as a function of La, Th composition. The magnetic susceptibility results are particularly interesting since they document the Ce impurity demagnetization directly. The diminution of the Ce magnetic moment with increasing Th concentration is evident in the inverse susceptibility vs temperature plots for various (La, Th)Ce alloys which are presented in Fig. 21.

Finally, it should be pointed out that a maximum in the initial depression of T_c with n, similar to that observed in the LaCe system under pressure and in the (La, Th)Ce system, has been observed in the (Zn, Al)Mn system [82]. A magnetic-nonmagnetic transition is expected here since the Mn moments are long-lived in the ZnMn system which has a Kondo temperature T_K of the order of ~0.2 K and short-lived in the AlMn system as noted in Subsection 1.3. It will be interesting to compare the various superconducting properties of the (Zn, Al)Mn system which are currently under investigation with those of the

(La, Th)Ce system; in particular, the evolution of the $\Delta C/\Delta C_0$ vs T_c/T_{c_0} curves with increasing Al composition. The only other systems in which measurements of $\Delta C/\Delta C_0$ vs T_c/T_{c_0} have been performed for different magnetic states of an impurity (corresponding to different compositions of the binary alloy matrix) are for (La, Y)Ce [84] and (Y, Th)Ce [92]. Unfortunately, both systems are not superconducting in the range of matrix compositions where the magnetic character of the Ce solutes is such that $\Delta T_c/n$ and $[d(\Delta C/\Delta C_0)/(T_c/T_{c_0})]_{T_c=T_{c_0}}$ might be expected to exhibit maxima. However, the trends are in good agreement with the behavior exhibited by the (La, Th)Ce system discussed above. When the composition of the La, Y matrix is varied toward Y in the (La, Y)Ce system, both $\Delta T_c/n$ and $[d(\Delta C/\Delta C_0/d(T_c/T_{c_0})]_{T_c=T_{c_0}}$ increase. This behavior suggests that T_K increases with Y concentration, which is in accord with expectations since T_K for the YCe system ($T_K \sim 40$ K) is much larger than for the LaCe system ($T_K \sim 0.1$ K). When the composition of the Y, Th matrix is varied towards Y in the (Y, Th)Ce system, again both $\Delta T_c/n$ and $[d(\Delta C/\Delta C_0)/d(T_c/T_{c_0})]_{T_c=T_{c_0}}$ increase. This behavior suggests that the spin fluctuation temperature T_0 decreases as the Y, Th composition is shifted away from pure Th towards Y, which, again, is in agreement with expectations since the Ce moments are long-lived in the YCe system and short-lived in the ThCe system.

3. Superconductors Containing Rare Earth Impurities with Crystal Field Split Energy Levels

As discussed in Subsection 1.2.1, the *temperature independent pair breaking* theory of Abrikosov and Gor'kov provides an excellent description of the superconducting properties of matrix-impurity systems in which the admixture of itinerant and local electron states is weak ($\vartheta > 0$) and the magnetic ground state of the impurity is separated from the excited states by temperatures which are very much larger than T_{c_0}. Calculations based on the AG theory predict that the curves of T_c/T_{c_0} vs n and $\Delta C/\Delta C_0$ vs T_c/T_{c_0} behave as universal functions for all matrix-impurity systems. This prediction has been borne out by experiment. However, if the $2J+1$ fold degeneracy of the Hund's rule ground state of the impurity ion is partially lifted by the crystalline electric field of the matrix, the resulting elastic and inelastic exchange scattering processes responsible for pair breaking are *temperature dependent*, even for $\vartheta > 0$. This is due to the fact that the relative populations of the ionic energy levels in the crystal field of the matrix are governed by the Boltzmann factor $f_i(T) = g_i \exp(-\delta_i/k_B T)$ where g_i is the degeneracy of level i and δ_i is its energy relative to the ground state. Temperature dependent pair breaking of this type, which has an entirely different origin than that encountered in Subsection 1.2.2 in connection with the Kondo effect, can still be calculated within the first Born approximation (to order ϑ^2) and depends on the detailed structure of the energy levels (degeneracies and splittings) in the crystal field. Physically, the most pronounced effects on the superconductivity of the matrix are expected when the splitting between the ground state and low lying excited states of the impurity are of the order of T_{c_0}.

In a recent series of papers, Fulde and coworkers developed a theory for the effect on superconductivity of paramagnetic RE impurities with crystal-field split energy levels [93–98]. According to this theory, the superconducting properties of the matrix are modified by two competing mechanisms. The first is a *depairing* mechanism involving the usual conduction electron-impurity spin exchange interaction which can be operative via off-diagonal matrix elements even when the relevant impurity energy levels are nonmagnetic. The second is a *pairing* mechanism (in addition to the electron-phonon interaction) which is associated with inelastic charge scattering of conduction electrons from the aspherical part of the $4f$ shell of the rare earth solute. Given the structure (i.e., splittings and degeneracies) of the energy levels of the rare earth impurity ions in the crystal field of the matrix, the theory admits to the calculation of various superconducting properties. In particular, Keller and Fulde have calculated numerically the behaviors of T_c/T_{c_0} vs n [94] and $\Delta C/\Delta C_0$ vs T_c/T_{c_0} [96] for various energy level schemes, neglecting, however, the pairing mechanism associated with aspherical Coulomb scattering. Calculations have also been made for the behavior of H_{c2} vs T [96], electron tunneling conductance [97] and the normal state thermoelectric power [98].

The earliest experiments on matrix-impurity systems with singlet ground states were made by Bucher *et al.* [99] and by Cooper [100]. Bucher *et al.* measured the T_c vs n curves for the cubic matrices $LaTl_3$, $LaSn_3$, $LaPb_3$, and Th with Pr and Tm impurities. It was found that the T_c vs n curves exhibited positive curvature much like that observed for the matrix-impurity systems with $T_0 \gg T_{c_0}$ discussed in Subsection 1.3. Recently, measurements of H_c vs T were made on the (LaTm)Sn_3 system by Guertin *et al.* [101]. All of

these investigations gave results in qualitative accord with the calculations of Fulde and coworkers. Cooper measured the magnetic susceptibility of the (LaTm)Al_2 system to determine the cubic crystal field parameters for Tm impurities in $LaAl_2$ which were then used to predict the crystal field energy level schemes for other RE impurities in $LaAl_2$ [100]. From data for $(-dT_c/dn)_{n=0}$ previously reported by Maple [102] for various RE impurities in $LaAl_2$, Cooper deduced the variation of $|\vartheta|$ with atomic number of the RE solute using the theory of Fulde *et al.* [93] and the predicted energy level schemes. In particular, Cooper's analysis indicated that Tb would have a singlet ground state in $LaAl_2$. This prediction has been verified experimentally by recent T_c vs n [103], H_{c2} vs T [103], $\Delta C/\Delta C_0$ vs T_c/T_{c_0} [104] and normal state thermoelectric power [105] measurements on the (LaTb)Al_2 system which also indicate that the lowest excited state of Tb is separated from the singlet ground state by ~ 5 K. Recent work has also included measurements of T_c vs n, H_{c2} vs T and $\Delta C/\Delta C_0$ vs T_c/T_{c_0} on the $(LaPr)_3In$ system [106], and T_c vs n and $\Delta C/\Delta C_0$ vs T_c/T_{c_0} on the $(LaPr)_3Tl$ system [107]. Many aspects of the theory of Fulde *et al.* appear to be satisfied, but problems remain, in particular, with respect to the detailed behavior of $\Delta C/\Delta C_0$ vs T_c/T_{c_0} which resembles the AG behavior for some systems (e.g., $(LaPr)_3In$ [106]) and the BCS behavior for others (e.g., (LaTb)Al_2 [104]) but does not conform to the behavior calculated by Keller and Fulde on the basis of the crystal field energy level scheme of the relevant impurity.

It should be emphasized that an understanding of the superconducting properties of matrices containing RE impurities with crystal field split energy levels provides a method for studying crystal field effects in metals. For example, measurements of T_c vs n under pressure in the (LaTb)Al_2 system [108, 109] have demonstrated that superconductivity studies under pressure provide a simple, yet effective, means of deducing shifts of the impurity energy levels with pressure.

As an exemplary matrix-RE impurity system where the crystal field splitting of the RE ion imparts particularly striking behavior to both the superconducting and normal state physical properties, we consider below the singlet ground state system (LaPr)Sn_3 which has recently been investigated by McCallum *et al.* [110]. For this system, the experimental T_c/T_{c_0} vs n and $\Delta C/\Delta C_0$ vs T_c/T_{c_0} curves are well represented by numerical calculations within the framework of the theory of Keller and Fulde, which are based on the energy level scheme of the Pr impurity ions as determined from separate measurements in the normal state.

3.1. *Exemplary System*—(LaPr)Sn_3

As an exemplary matrix-impurity system in which the crystal field splitting of the Hund's rule multiplet results in a singlet ground state, we consider the system (LaPr)Sn_3 which has recently been studied in both the superconducting and normal states. In the superconducting state, the variations of T_c/T_{c_0} with n and $\Delta C/\Delta C_0$ with T_c/T_{c_0} have been measured in detail [110] and the results are shown in Figs. 22 and 23, respectively. The curve of T_c/T_{c_0} vs n exhibits the positive curvature which is characteristic of many matrix-impurity systems with singlet impurity ground states, while the curve of $\Delta C/\Delta C_0$ vs T_c/T_{c_0} shows a pronounced deviation from both the BCS and AG curves which has not heretofore been observed. As discussed in the preceding sections, the $\Delta C/\Delta C_0$ vs T_c/T_{c_0} curve generally lies on or below the BCS curve, but not above it as observed here.

The striking results shown in Figs. 22 and 23 can be described quite well by calculations based on the theory of Keller and Fulde, which are represented by the solid lines in the figures. The theoretical T_c/T_{c_0} vs n curve has been fitted to the experimental data at low concentrations, while the theoretical $\Delta C/\Delta C_0$ vs T_c/T_{c_0} curve has no adjustable parameters. Both of the

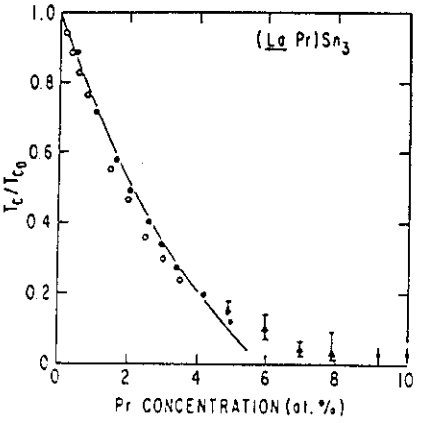

Fig. 22. Reduced transition temperature T_c/T_{c_0} vs Pr concentration for the (LaPr)Sn_3 system. The open and solid symbols represent data taken at Bell Laboratories and the University of California, San Diego, respectively. The solid line is derived from numerical calculations based on the theory of Keller and Fulde [94] with $(dT_c/dn)_{n=0}$ as the only adjustable parameter (after McCallum *et al.* [110])

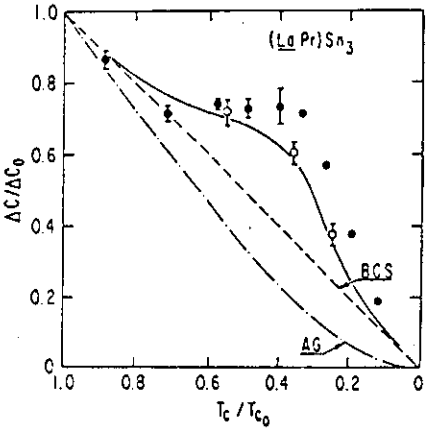

Fig. 23. Reduced specific heat jump $\Delta C/\Delta C_0$ vs reduced transition temperature T_c/T_{c_0} for the (La Pr)Sn_3 system. The open and solid symbols have the same meaning as in Fig. 22. The solid line is derived from numerical calculations based on the theory of Keller and Fulde [96] with no adjustable parameters. The BCS curve (dashed line) and AG curve (dot-dashed line) are shown for comparison (after McCallum *et al.* [110])

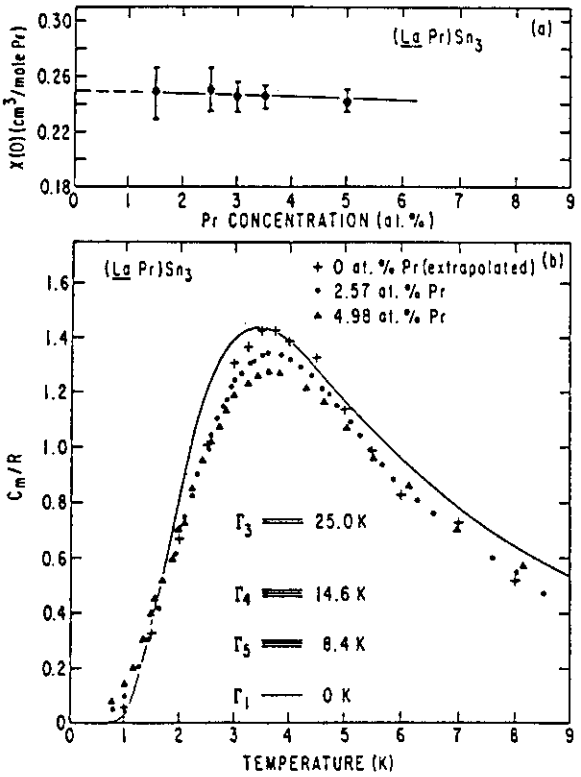

Fig. 24. (a) Zero temperature magnetic susceptibility $\chi(0)$ vs Pr concentration for the (La Pr)Sn_3 system. (b) Excess specific heat C_m/R vs temperature for the (La Pr)Sn_3 system for impurity concentrations of 0 (extrapolated), 2.57 and 4.98 at.-% Pr. The solid line represents the best fit of the theoretical Schottky function to the extrapolated zero Pr concentration data corresponding to the Pr energy level scheme indicated in the figure (after McCallum *et al.* [110])

calculated curves, which are in relatively good agreement with experiment, are based on the Pr^{3+} energy level structure in the cubic crystal field of the $LaSn_3$ matrix which was determined from measurements in the normal state of the Van Vleck paramagnetic susceptibility and Schottky heat capacity anomaly for various Pr concentrations [110]. A plot of the zero temperature magnetic susceptibility $\chi(0)$ vs Pr concentration is presented in Fig. 24a, while typical data for the excess heat capacity C_m/R vs temperature are shown in Fig. 24b for Pr concentrations of 2.57 and 4.98 at.-%. These data were extrapolated to zero Pr concentration, as indicated in Figs. 24a and 24b, to attain an estimate of the value of $\chi(0)$ and the behavior of C_m/R vs T in the single Pr impurity limit. Using the energy level diagram of Lea *et al.* [111] for Pr^{3+} in a cubic crystal field, theoretical expressions for $\chi(0)$ and $C_m(T)/R$ were then fitted to the data in the single Pr impurity limit. The best fit corresponds to the following Pr^{3+} energy level scheme: Γ_1 (singlet) -0 K, Γ_5 (triplet) -8.4 K, Γ_4 (triplet) -14.6 K, and Γ_3 (doublet) -25.0 K.

The good agreement between the calculated and experimental curves in Figs. 22 and 23 indicates that pairing due to aspherical Coulomb scattering, which has been neglected in the calculations of Keller and Fulde, is not an important effect, except possibly above ~ 4 at.-% Pr where the data depart from the theoretical curve. This is consistent with theoretical expectations since the splitting δ_{15} between the singlet Γ_1 ground state and the triplet Γ_5 excited state must be $\gtrsim 6\,T_c$ for Γ_1–Γ_5 transitions to be effective in enhancing T_c by aspherical Coulomb scattering according to [93]. Thus one expects to observe this effect only for $T_c/T_{c_0} \lesssim 0.2$ which corresponds to the Pr concentration range above ~ 4 at.-%. Although these results are suggestive, it is clear that more experimentation is required before the existence of pairing by aspherical Coulomb scattering can be firmly established. The measurements on the (La Pr)Sn_3 system reviewed here show that matrices which contain RE impurities with crystal field split energy levels exhibit striking superconducting properties which can be accounted for in terms of elastic and inelastic exchange scattering processes.

In addition to these zero pressure studies, the dependence of T_c on pressure has recently been

measured for the (La Pr)Sn_3 system by DeLong *et al.* [112]. In contrast to the results obtained for the singlet ground state (La Tb)Al_2 system [108, 109], the depression of T_c was found to *increase* with increasing pressure for the (La Pr)Sn_3 system. From this behavior it can be inferred that $|\mathcal{J}|$ increases anomalously with pressure and/or the energy separating the crystal field levels decreases with pressure. The first alternative suggests that $\mathcal{J}$ is dominated by an admixture contribution, while the second implies a breakdown of the point charge model.

4. Conclusions

The experiments reviewed herein show that impurities with partially-filled d or f shells impart many varied and striking behaviors to the superconducting properties of the matrices into which they have been dissolved. In particular, the impurity ions affect the superconducting state in a distinct manner which correlates with their own magnetic state. The two distinguishing features we have emphasized in this review are the *detailed* behavior of the curves of T_c/T_{c_0} vs n and $\Delta C/\Delta C_0$ vs T_c/T_{c_0}, although other properties could be utilized such as the dependence of the critical magnetic field on temperature and impurity concentration or electron tunneling characteristics. We have chosen to focus on the curves of T_c/T_{c_0} vs n and $\Delta C/\Delta C_0$ vs T_c/T_{c_0} since the measurements are relatively easy to perform and, as we have shown, the detailed shapes of the curves are extremely sensitive to the magnetic state of the impurity. From the evidence presented, it is apparent that the systematics of superconductivity in the presence of local moments are sufficiently well established to allow the magnetic state of an impurity to be determined from superconducting properties alone. Specifically, we have shown that it is possible to 1) ascertain whether the solute spin is long-lived (magnetic) or short-lived (nonmagnetic) compared to thermal fluctuation lifetimes at superconducting temperatures, 2) determine the sign and magnitude of the conduction electron-impurity spin exchange interaction parameter $\mathcal{J}$ and the temperature dependence of the exchange scattering of conduction electrons by *long-lived* solute spins, 3) derive, in favorable cases, information pertaining to the energy level structure of rare earth ions in the crystalline electric field of their superconducting metallic host, and 4) observe magnetic-nonmagnetic transitions of an impurity induced by the application of an external pressure or variation of the composition of a binary alloy matrix.

References

1. M. B. Maple: AIP Conf. Proc. (No. 4) Superconductivity in *d*- and *f*-Band Metals, ed. by D. H. Douglass, pp. 175–203 (1972)
2. M. B. Maple: In *Magnetism: A Treatise on Modern Theory and Materials*, ed. by H. Suhl (Academic Press, New York 1973) Vol. V, Chapter 10
3. E. Müller-Hartmann: In *Magnetism: A Treatise on Modern Theory and Materials*, ed. by. H. Suhl (Academic Press, New York 1973) Vol. V, Chapter 12
4. C. Rizzuto: Rep. Prog. Phys. 37, 147 (1974)
5. C. F. Ratto: Rivista Nuovo Cimento 2, 203 (1972)
6. J. Friedel: Nuovo Cimento Suppl. 12, 1861 (1958)
7. P. W. Anderson: Phys. Rev. 124, 41 (1961)
8. A. J. Heeger: Solid State Phys. 23, 283 (1969)
9. See various articles in *Magnetism: A Treatise on Modern Theory and Materials*, ed. by H. Suhl (Academic Press, New York 1973) Vol. V
10. L. L. Hirst: Phys. Kondens. Mat. 11, 255 (1970)
11. M. B. Maple, D. Wohlleben: Phys. Rev. Letters 27, 511 (1971)
12. M. B. Maple, D. Wohlleben: AIP Conf. Proc. (No. 18) on "Magnetism and Magnetic Materials – 1973", ed. by C. D. Graham, Jr. and J. J. Rhyne (1974) pp. 447–462
13. M. B. Maple, J. G. Huber, K. S. Kim: Solid State Commun. 8, 981 (1970)
14. J. G. Huber, M. B. Maple: J. Low Temp. Phys. 3, 537 (1970)
15. P. G. deGennes: J. Phys. Rad. 23, 510 (1962)
16. H. Suhl, B. T. Matthias: Phys. Rev. 114, 977 (1959)
17. M. B. Maple: Ph. D. Thesis, University of California, San Diego, La Jolla, California (1969) (unpublished)
18. M. B. Maple: Solid State Commun. 12, 653 (1973)
19. D. Davidov, A. Chelkowski, C. Rettori, R. Orbach, M. B. Maple: Phys. Rev. B 7, 1029 (1973)
20. M. B. Maple: Phys. Letters 26A, 513 (1968)
21. C. A. Luengo, M. B. Maple: Solid State Commun. 12, 757 (1973)
22. A. A. Abrikosov, L. P. Gor'kov: Zh. Eksp. Teor. Fiz. 39, 1781 (1960); — Sov. Phys. JETP 12, 1243 (1961)
23. W. R. Decker, D. K. Finnemore: Phys. Rev. 172, 430 (1968)
24. S. Skalski, O. Betbeder-Matibet, P. R. Weiss: Phys. Rev. A136, 1500 (1964)
25. J. Bardeen, L. N. Cooper, J. R. Schrieffer: Phys. Rev. 108, 1175 (1957)
26. P. W. Anderson, A. M. Clogston: Bull. Am. Phys. Soc. 6, 124 (1961). — J. Kondo: Progr. Theoret. Phys. (Kyoto) 28, 846 (1962). — P. G. deGennes: J. Physique 23, 630 (1962)
27. J. R. Schrieffer, P. A. Wolff: Phys. Rev. 149, 491 (1966)
28. For reviews, see J. Kondo: Solid State Phys. 23, 183 (1969) and Refs. [8] and [9]
29. J. Kondo: Progr. Theoret. Phys. 32, 37 (1964)
30. M. B. Maple, Z. Fisk: Proc. Int. Conf. Low Temp. Phys., 11th, St. Andrews, Scotland, 1968, ed. by J. F. Allen, D. M. Finlayson, and D. M. McCall, Vol. 2, pp. 1288–1292, St. Andrews, Scotland (1968)
31. J. A. White, H. J. Williams, J. H. Wernick, R. C. Sherwood: Phys. Rev. 131, 1039 (1963)
32. R. Harris, M. J. Zuckermann: To be published
33. W. Felsch, K. Winzer, G. v. Minnigerode: Z. Physik B21, 151 (1975)
34. S. D. Bader, N. E. Phillips, M. B. Maple, C. A. Luengo: Solid State Commun. 16, 1263 (1975)
35. S. D. Bader: Ph. D. Thesis, University of California, Berkeley, California (1974) (unpublished)
36. P. E. Bloomfield, D. R. Hamann: Phys. Rev. 164, 856 (1967)
37. K. Winzer: Z. Physik 265, 139 (1973)

38. J. H. Moeser, F. Steglich, G. v. Minnigerode: J. Low Temp. Phys. 15, 91 (1974)
39. A. Benoit, J. Flouquet, J. Sanchez: Solid State Commun. 13, 1581 (1973)
40. G. Riblet, K. Winzer: Solid State Commun. 9, 1663 (1971)
41. M. B. Maple, W. A. Fertig, A. C. Mota, L. E. DeLong, D. Wohlleben, R. Fitzgerald: Solid State Commun. 11, 829 (1972)
42. C. A. Luengo, M. B. Maple, W. A. Fertig: Solid State Commun. 11, 1445 (1972)
43. H. Armbrüster, H. v. Löhneysen, G. Riblet, F. Steglich: Solid State Commun. 14, 55 (1974)
44. F. Steglich, H. Armbrüster: Solid State Commun. 14, 903 (1974)
45. T. Aoi, Y. Masuda: J. Phys. Soc. Japan 37, 673 (1974)
46. F. W. Smith: J. Low Temp. Phys. 5, 683 (1971)
47. R. Vaccarone, A. Morozzo della Rocca, A. Pilot, F. Vivaldi, C. Rizzuto: Solid State Commun. 12, 885 (1973)
48. S. Takayanagi, M. Takano, Y. Kimura, T. Sugawara: J. Low Temp. Phys. 16, 519 (1974)
49. P. Fulde, K. Maki: Phys. Rev. 141, 275 (1966)
50. M. J. Zuckermann: Phys. Rev. 168, 390 (1968)
51. E. Müller-Hartmann, J. Zittartz: Z. Physik 234, 58 (1970)
52. E. Müller-Hartmann, J. Zittartz: Solid State Commun. 11, 401 (1972)
53. E. Müller-Hartmann, J. Zittartz: Phys. Rev. Letters 26, 428 (1971)
54. A. Ludwig, M. J. Zuckermann: J. Phys. F1, 516 (1971)
55. P. Schlottmann: Solid State Commun. 16, 1297 (1975); — J. Low Temp. Phys. 20, 123 (1975)
56. P. M. Chaikin, T. W. Mihalisin: Solid State Commun. 10, 465 (1972); — Phys. Rev. B6, 839 (1972)
57. J. J. Préjean, J. Souletie, J. Teixeira: J. Phys. F5, L6 (1975)
58. M. B. Maple, J. G. Huber, B. R. Coles, A. C. Lawson: J. Low Temp. Phys. 3, 137 (1960)
59. C. A. Luengo, J. M. Cotignola, J. Sereni, A. R. Sweedler, M. B. Maple, J. G. Huber: Solid State Commun. 10, 459 (1972)
60. C. A. Luengo, J. M. Cotignola, J. Sereni, A. R. Sweedler, M. B. Maple: Proc. 13th Int. Conf. Low Temp. Phys., Boulder, Colorado (1972), ed. by K. D. Timmerhaus, W. J. O'Sullivan, and E. F. Hammel (Plenum Press, New York, London 1972) pp. 585–589
61. R. P. Guertin: Ph. D. Thesis, University of Rochester, Rochester, New York (1968) (unpublished)
62. J. G. Huber, M. B. Maple: Solid State Commun. 8, 1987 (1970)
63. A. B. Kaiser: J. Phys. C3, 409 (1970)
64. H. L. Watson, D. T. Peterson, D. K. Finnemore: Phys. Rev. B8, 3179 (1973)
65. F. W. Smith: J. Low Temp. Phys. 6, 435 (1972)
66. D. L. Martin: Proc. Soc. (London) 78, 1489 (1961)
67. C. W. Dempesy: Private communication of unpublished data (1970); reported in Ref. [14]
68. M. J. Zuckermann: Phys. Rev. A140, 899 (1965)
69. C. F. Ratto, A. Blandin: Phys. Rev. 156, 513 (1967)
70. K. Takanaka, F. Takano: Progr. Theor. Phys. 36, 1080 (1966)
71. J. R. Schrieffer, L. Mattis: Phys. Rev. A140, 1412 (1965)
72. J. Rössler, M. Kiwi: Phys. Rev. B10, 95 (1974)
73. M. B. Maple, K. S. Kim: Phys. Rev. Letters 23, 118 (1969)
74. M. B. Maple, J. Wittig, K. S. Kim: Phys. Rev. Letters 23, 1375 (1969)
75. S. DeGennaro, E. Borchi: Phys. Rev. Letters 30, 377 (1973). — A. S. Edelstein: Phys. Rev. Letters 20, 1348 (1968)
76. Consult [1] and [2] and references cited therein
77. K. S. Kim, M. B. Maple: Phys. Rev. B2, 4696 (1970)
78. B. Coqblin, M. B. Maple, G. Toulouse: Int. J. Magn. 1, 333 (1971)
79. W. Gey, E. Umlauf: Z. Physik 242, 241 (1971)
80. M. B. Maple, J. Wittig: Solid State Commun. 9, 1611 (1971)
81. M. Dietrich, W. Gey, E. Umlauf: Solid State Commun. 11, 655 (1972)
82. G. Boato, C. Rizzuto: Proc. Int. Conf. Low Temp. Phys., 11th, St. Andrews, Scotland (1968), ed. by J. F. Allen, D. M. Finlayson, and D. M. McCall, St. Andrews, Scotland (1968) Vol. 2, pp. 1062–1065
83. J. G. Huber, M. B. Maple: Proc. 13th Int. Conf. Low Temp. Phys., Boulder, Colorado (1972), ed. by K. D. Timmerhaus, W. J. O'Sullivan, and E. F. Hammel (Plenum Press, New York, London 1972) pp. 579–584
84. T. Aoi, J. Takeuchi, Y. Masuda: J. Phys. Soc. Japan 36, 1485 (1974)
85. S. Ortega, M. Roth, C. Rizzuto, M. B. Maple: Solid State Commun. 13, 5 (1973)
86. J. G. Huber, W. A. Fertig, M. B. Maple: Solid State Commun. 15, 453 (1974)
87. C. A. Luengo, J. G. Huber, M. B. Maple, M. Roth: Phys. Rev. Letters 32, 54 (1974)
88. C. A. Luengo, J. G. Huber, M. B. Maple, M. Roth: J. Low Temp. Phys. 21, 129 (1975)
89. V. Jaccarino, L. R. Walker: Phys. Rev. Letters 15, 258 (1965)
90. O. Peña, F. Meunier: Solid State Commun. 14, 1087 (1974)
91. J. G. Huber, J. Brooks, D. Wohlleben, M. B. Maple: AIP Conf. Proc. (No. 24) on "*Magnetism and Magnetic Materials* – 1974" ed. by C. D. Graham, Jr., G. H. Lander, and J. J. Rhyne (1975) pp. 475–476
92. J. Sereni: Private communication
93. P. Fulde, L. L. Hirst, A. Luther: Z. Physik 230, 155 (1970). — P. Fulde, H. E. Hoenig: Solid State Commun. 8, 341 (1970)
94. J. Keller, P. Fulde: J. Low Temp. Phys. 4, 289 (1971)
95. P. Fulde, I. Peschel: Advan. Phys. 21, 1 (1972)
96. J. Keller, P. Fulde: J. Low Temp. Phys. 12, 63 (1973)
97. P. Holzer, J. Keller, P. Fulde: J. Low Temp. Phys. 14, 247 (1974)
98. I. Peschel, P. Fulde: Z. Physik 238, 99 (1970)
99. E. Bucher, K. Andres, J. P. Maita, G. W. Hull: Helv. Phys. Acta 41, 723 (1968)
100. J. R. Cooper: Solid State Commun. 9, 1429 (1971)
101. R. P. Guertin, J. E. Crow, A. R. Sweedler, S. Foner: Solid State Commun. 13, 25 (1973)
102. M. B. Maple: Solid State Commun. 8, 1915 (1970)
103. G. Pepperl, E. Umlauf, A. Meyer, J. Keller: Solid State Commun. 14, 161 (1974)
104. H. Happel, H. E. Hoenig: Solid State Commun. 13, 1641 (1973)
105. E. Umlauf, G. Pepperl, A. Meyer: Phys. Rev. Letters 30, 1173 (1973)
106. F. Heiniger, E. Bucher, J. P. Maita, L. D. Longinotti, A. S. Cooper, P. Descouts: To be published (reported in [95])
107. E. Bucher, J. P. Maita, A. S. Cooper: Phys. Rev. B6, 2709 (1972)
108. R. P. Guertin, W. Bolvin, J. E. Crow, A. R. Sweedler, M. B. Maple: Solid State Commun. 13, 1889 (1973)
109. E. Umlauf, P. Holzer, J. Keller, M. Dietrich, W. Gey, R. Meier: Z. Physik 271, 305 (1974)
110. R. W. McCallum, W. A. Fertig, C. A. Luengo, M. B. Maple, E. Bucher, J. P. Maita, A. R. Sweedler, L. Mattix, P. Fulde, J. Keller: Phys. Rev. Letters 34, 1620 (1975)
111. K. R. Lea, M. J. Leask, W. P. Wolf: J. Phys. Chem. Solids 23, 1381 (1962)
112. L. E. DeLong, R. W. McCallum, M. B. Maple: Proc. 14th Int. Conf. on Low Temperature Physics, Helsinki, Finland (1975)